International Journal of Coal Geology 212 (2019) 103202

Contents lists available at ScienceDirect

International Journal of Coal Geology

journal homepage: www.elsevier.com/locate/coal

Comparative study on sorption characteristics of coal seams from Barakar and Raniganj formations of Damodar Valley Basin, India

Sujoy Chattaraj[a,b], Debadutta Mohanty[a,*], Tarkeshwar Kumar[c], Gopinath Halder[b], Kanhaiya Mishra[a]

[a] Non-Conventional Gases Section, CSIR – Central Institute of Mining and Fuel Research, Dhanbad 826 015, India
[b] Department of Chemical Engineering, National Institute of Technology Durgapur, Durgapur 713 209, India
[c] Department of Petroleum Engineering, IIT-Indian School of Mines, Dhanbad 826 004, India

ARTICLE INFO

Keywords:
Sub-basin
Thermal history
Methane
Sorption
Micropores

ABSTRACT

The methane retention mechanism in coal seams is markedly different from those of conventional gas reservoirs. Methane remains mainly as physically adsorbed molecules on micropore surface. Chemical and petrographic compositions of coal are the measures of maturity and type of organic matter that control the methane sorption characteristics of the coal. 99% of Indian coal occurrences are contributed by lower Gondwana sequences housed in two major geologic formations, younger Raniganj and older Barakar. The Raniganj Formation is best exposed in Raniganj Sub-basin and Barakar Formation is best exposed in Jharia Sub-basin of Damodar Valley. Present work attempts a systematic investigation on comparative account of methane sorption characteristics of coals from Raniganj Formation of Raniganj Sub-basin and Barakar Formations of Jharia Sub-basin in relation to their chemical composition and petrographic makeup. Chemical analyses shows that moisture, ash, volatile matter and fixed carbon varies between 2.5 and 4.6%, 10.0–27.2%, 38.8–40.2% (dmmf) and 59.8–61.2% (dmmf), respectively for Raniganj coals and, 0.5–1.1%, 16.7–32.9%, 20.7–22.0% (dmmf) and 78.0–79.3% (dmmf), respectively for Barakar coals. Carbon content is distinct for the suites of coal, 79.2–85.4% and 85.6–92.0% for Raniganj and Barakar coals, respectively. The vitrinite reflectance for the Raniganj coals ranges 0.53–0.72% and the Barakar coals ranges 1.09–1.23%. Based on the chemical composition and vitrinite reflectance value Raniganj coals belongs to high volatile bituminous type, whereas Barakar coals belongs to high to medium volatile bituminous type. Such variation in composition and maturity is mainly attributed to the variation in precursor organic matter as well as the basinal and thermal history of the sub-basins under consideration.

H/C atomic ratio of the Raniganj and Barakar coals varies between 0.65 and 0.80 and 0.51–0.72 and O/C atomic ratio varies between 0.05 and 0.13 and 0.01–0.07, respectively. Coals of both the Raniganj and Barakar formations are mostly of kerogen Type-III with Raniganj coals falling in wet gas maturity stage approaching early-thermogenic methane generation whereas Barakar coals falling in condensate gas stage approaching peak-thermogenic methane generation. The Langmuir volume ranges from 9.3–21.8 cc/g (daf) for Raniganj coals and 21.1–29.1 cc/g (daf) for Barakar coals. Sorption capacity for the set of coals shows a strong rank dependency and increase with corresponding increase in rank down the stratigraphic column. Methane sorption capacity shows positive relationship with carbon content and vitrinite reflectance, and negative relationship with moisture content, ash and volatile matter. Moisture effect is more prominent in low rank Raniganj coals. The adsorption capacity shows a strong positive relation with vitrinite content and a moderate negative relation with inertinite content for both the Raniganj and Barakar coals, which may be attributed to dominancy of micropores in vitrinites with rank enhancement. The multiple regression analysis shows that the moisture is the main predictor of the V_L, and the interaction of moisture with ash and reflectance mainly control the sorption capacity. A predictive model equation is developed for determination of sorption for Damodar basin coals from carbon, ash and moisture data.

* Corresponding author.
E-mail address: drdmohanty@ymail.com (D. Mohanty).

https://doi.org/10.1016/j.coal.2019.05.009
Received 15 November 2018; Received in revised form 7 May 2019; Accepted 13 May 2019
Available online 15 May 2019
0166-5162/

1. Introduction

The methane generated during the coalification process remains trapped within the coal seams and associated rocks are known as coalbed methane. The gas retention mechanism in coal seams is markedly different from that of conventional oil and gas reservoirs. Coal seam gases are generally found as adsorbed molecules on surface, absorbed gas within the matrix, free gas in cleats and fractures, and as a solute in ground water (Murray, 1991). However, physical adsorption is the dominant mechanism governing the storage of CBM in the coal seam (Crosdale et al., 1998). USA, China, Australia and Canada are the major CBM producing countries having CBM resources locked up in the coals of different age and rank. Coal bearing Upper Cretaceous Fruitland Formation of San Juan basin and Cretaceous Pottsville Formation of Black Warrior basin are the principal CBM producing zones of USA. Alberta Basin hosts the major hydrocarbon resources in Canada. These coals from Cretaceous to Tertiary strata are similar to Rocky mountain foreland basin of USA. High permeable thin coal seams of Jurassic Walloon Coal Measures of Surat Basin and relatively thick coal seams of Permian Baralaba Coal Measures and Bandanna formation of Bowen Basin are the principle gas producing horizons in Australia (Towler et al., 2016). Qinshui and Ordos basins are the key CBM producing areas in China, accounting for 94.6% of the total production in 2014. Carboniferous Benxi and Taiyuan Formations in the Ordos basin and Permian Shanxi Formation and Carboniferous Taiyuan Formation in Qinshui basin of China are the major coal bearing strata (Mu et al., 2015). Hence, it is important to investigate the CBM potentiality of different coal basins in terms of their age, rank, types, grades etc. in the light of their chemical and petrographic makeup.

The total prognosticated CBM resource of India from 33 CBM blocks awarded in four rounds of bidding is about 1767 BCM (DGH, 2019) that includes Permian coal basins of Damodar valley, Son Valley, Tertiary coal basins of North East India, Tertiary Neyveli lignites etc. The coalfields of Damodar (Raniganj, Jharia, Bokaro & North Karanpura) and Son River Valley (Sohagpur) have emerged as the most prospective for CBM exploration and 8 blocks in these two river valley Basins are in the development phase with an estimated gas-in-place of 280 BCM (DGH, 2019). However, these blocks are yet to enter into the commercial exploitation phase. The coal measures of India belong to two broad geologic periods, Permian and Tertiary. The Permian Lower Gondwana sequences of Peninsular India hosts almost 99% of the Country's coal resource. Gondwana coal basins are distributed along three major river valley lineaments, the Damodar Valley, Son-Mahanadi Valley and Godavari Valley (Fig. 1a-*i*). The east–west trending Damodar Valley hosts major prime coking coal reserves of the country and is a main coalfield for CBM exploration. A major normal fault that runs the length of the Damodar Valley marks the southern edge of the major coalfields where Gondwana sediments are in contact with the Precambrian gneissic terrain (Fig. 1a-*ii*). The intra-basinal faulting and igneous activity have complicated the structure of the Damodar Valley basin. During the Permian period, coal seams were most likely formed throughout the entire Damodar Valley. Subsequent upliftment and erosion of the Gondwana sediments, however, has left only the isolated coalfields now preserved as graben and half-graben structures in Damodar Valley, from east to west, namely Raniganj, Jharia, East and West Bokaro, Ramgarh, South and North Karanpura coalfields. The strata generally dip towards the faulted southern boundary.

The chemical and petrographic composition of coal, rank and the type of organic matter are the main factors controlling the amount of gas adsorbed in coals (Chattaraj et al., 2016). Extensive study on sorption behavior of coals from different parts of the globe has been carried out in relation to CBM exploration. Though these studies have added to our understanding about coalbed methane, there is strong need to assess the CBM potentiality of particular basin in terms of its source organic matter, basinal and thermal history (Busch and Gensterblum, 2011; Chattaraj et al., 2016). Hence, an attempt is made to study the sorption behavior of the coals from the two major coal-bearing formations of two different sub-basins of Damodar Valley, India, Raniganj Formation of Raniganj Sub-basin and Barakar formation of Jharia Sub-basin under same experimental conditions. Further, efforts were made to correlate the adsorption capacity of the coals with their chemical composition, petrographic makeup and maturity.

2. Geology of the study area

The Lower Gondwana sequence of India is comprised of five formations namely Talchir, Karharbari, Barakar, Barren Measure and Raniganj from bottom to top. Among them Karharbari is almost missing in the Damodar Valley, except in the Giridih Gondwana sub-basin. The Damodar Valley Basin is regarded as an 'outlier' in the Archaean country. Overlying the Talchir formation, Damuda group holds the major coal resources and is classified into three distinct formations viz. Barakar, Barren Measures and Raniganj (Fig. 2) with a cumulative thickness of nearly 2500 m. The Barren Measures is not a coal-bearing formation and separates the underlying Barakar and overlying Raniganj coal bearing formations (Dutta, 2002). Coal seams occur both in the Barakar and in Raniganj Formations. The Barakar formation is best exposed in the Jharia Sub-basin and is the sole repository of prime coking coals in the country. The Raniganj Formation is best developed in the Raniganj Sub-basin and their importance diminishes towards west in the Damodar Valley and in rest of the peninsular India.

2.1. Raniganj sub-basin

Raniganj Sub-basin spreading over an area of 1550 km^2 is the eastern most member of Damodar Valley Coalfields bounded by the latitudes 23°03′:23°52′N and longitudes 86°25′:87°37′E. Two prominent elevations namely, Panchet and Biharinath are conspicuous in the southern part of the Sub-basin. Three perennial rivers Ajay, Barakar and Damodar along with their tributaries drain the northern, eastern and southern parts of the Sub-basin. The Coalfield has a semi-elliptical elongated shape and is bounded on the north, west and south by the Archaean metamorphics except in the east, where it is covered by alluvium. Archaean metamorphic rocks consisting of granite gneiss, migmatite gneiss, hornblende schist, hornblende gneiss, metabasic rocks, pegmatite and quartz veins etc. represent basement of Raniganj coalfield. Though several correlations are available for the regional as well as local coal seams of Raniganj Formation, the one generally accepted, recognizes ten groups of coal seams numbered R-I to R-X in the ascending order.

2.2. Jharia sub-basin

The Jharia Sub-basin is the second eastern most member of the Damodar Valley basin banked by the Raniganj Sub-basin in the east and Bokaro Sub-basin in the west. The Jharia Sub-basin is a sickle-shaped synclinal basin with an east-west alignment. The Sub-basin is extended over an area of about 453km^2 bounded by latitudes 23°37′:23°52′N and longitudes 86°06′:86°30′E lying mostly in the Dhanbad district of Jharkhand. It is an outlier of Permo-Carboniferous lower Gondwana sediments in an Archaean country. The area is mostly covered with alluvial soil and successive outcrops of older rocks from north to south and Barren measures outcrop at the central part. The coal seams occur in the Jharia Sub-basin in both Barakar and Raniganj Formation though workable coal seams are present only in Barakar Formation. As far as the number of coal seams (50 cm and more in thickness) is concerned, the existence of as many as 46 (including 5 local) seams in Barakar Measures and 24 (including 4 local) seams in Raniganj Measures have been proved. Out of the above-mentioned Barakar coal measures, 18 coal seams (I to XVIII) have been identified as regionally correlatable coal seams (Fox, 1930).

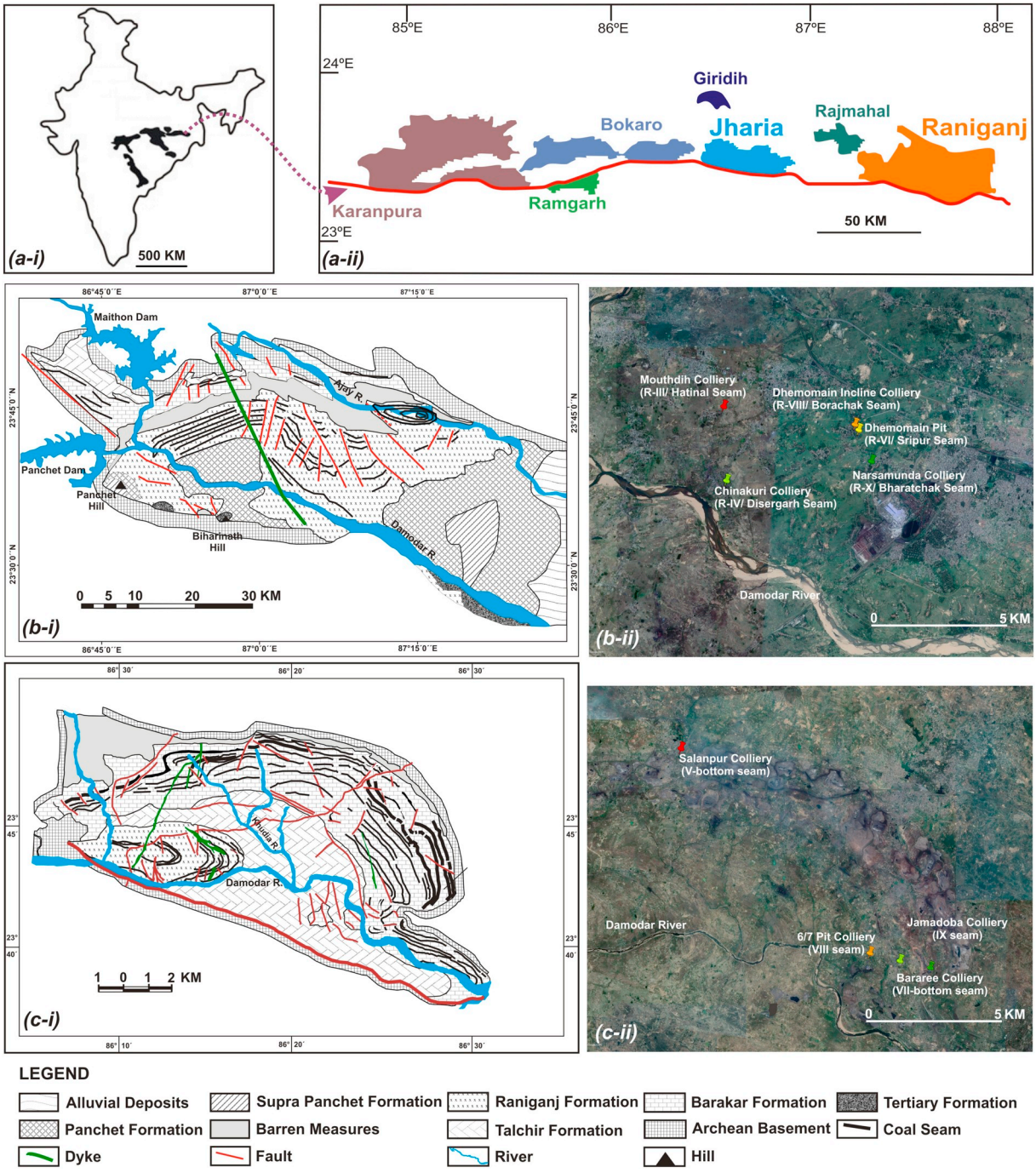

Fig. 1. Map showing *(a-i)* distribution of Permian Gondwana coalfields of India, *(a-ii)* coalfields of Damodar Valley basin *(b-i)* geological map of Raniganj Sub-basin *(b-ii)* Google Earth image of Raniganj Sub-basin with sample locations *(c-i)* geological map of Jharia Sub-basin *(c-ii)* Google Earth image of Jharia Sub-basin with sample locations.

3. Materials and methods

Channel samples were collected from the different underground mines of Raniganj and Jharia Sub-basins. Narsamuda, Dhemomain (incline and pit), Chinakuri and Mouthdih collieries were visited in the Raniganj Sub-basin for sample collection. Jamdadoba, Bhutgoria (6/7 pit), Bararee and Salanpur collieries were visited for the sample collection in the Jharia Sub-basin. Two channel samples for the entire exposed thickness were collected for each coal seam (as A and B) from the respective collieries, and 6–8 kg coal were used to prepare composite samples for each channel for the purpose of the present investigation. Detailed location of the sample sites are presented in Table 1. ASTM D2013/D2013M (2018) standard was followed for the sample preparation of proximate, ultimate and adsorption isotherm analysis and ISO 7404-2 (1985) was followed for the sample preparation of petrographic analyses. The samples were analyzed for proximate, elemental and petrographic composition, and adsorption isotherm construction. The work plan for the present investigation is presented in the flow diagram (Fig. 3).

3.1. Proximate analyses

Approximately, 250 g of samples were prepared to −60 BSS mesh (−250 μm) size for proximate analysis that includes ash, moisture,

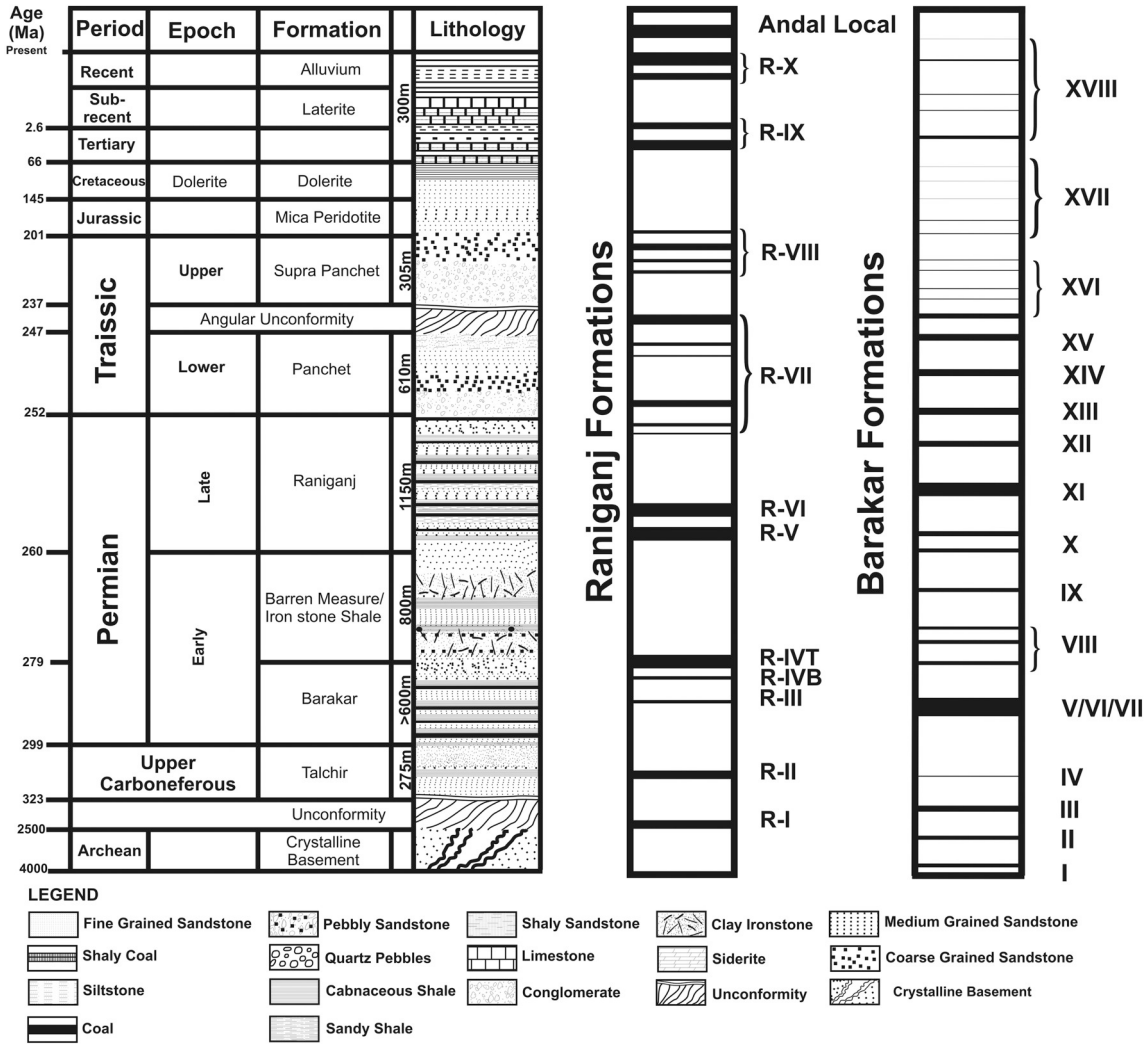

Fig. 2. Generalized stratigraphic sequence of Damodar Valley basin and coal seam sequences in older Barakar and younger Raniganj Formations (modified after Raja Rao, 1983; Veevers and Tiwari, 1995).

volatile matter and fixed carbon following ASTM D3172 (2013). The results of proximate analysis are reported as weight percentage of the air-dried material. Fixed carbon is estimated by deducting the sum total of percentages of ash, moisture and volatile matter from 100 i.e., Fixed carbon (FC) = 100 – (A + M + VM). Volatile matter and fixed carbon are expressed on dry ash-free basis (daf).

3.2. Elemental analysis

−60 BSS mesh (−250 μm) size sample was for the ultimate analysis. The analysis includes the determination of carbon, hydrogen, sulfur and nitrogen in the material, as found in the gaseous products on its complete combustion and the calculation of oxygen by difference. Ultimate analysis was done using Elementar make Vario Macrocube

Table 1
Detailed information of the location of the sample collection.

Sample ID/seam[a]	Colliery	Location	Latitude/longitude
Raniganj formation/Raniganj sub-basin			
R-X (A&B)	Narsamuda	Sec 4, 17WL/19R	23°41′24.35″N, 86°54′53.63″E
R-VIII (A&B)	Dhemomain incline	74EL/13D	23°42′10.13″N, 86°54′31.25″E
R-VI (A&B)	Dhemomain Pit	-2 L/15R	23°42′3.37″N, 86°54′36.37″E
R-IV (A&B)	Chinakuri 1 No.	0&1 L central drift	23°41′0.23″N, 86°51′36.64″E
R-III (A&B)	Mouthdih	49.5 L/9&10D	23°42′32.49″N, 86°51′32.92″E
Barakar formation /Jharia sub-basin			
B-XI (A&B)	Jamadoba	2 L/−7R	
B-IX (A&B)	Bhutgoria 6/7 pit	15D/0/5LN	23°42′11.82″N, 86°24′57.87″E
R-VIII (A&B)	Bhutgoria 6/7 pit	4R/3 L	
B-VII (A&B)	Bararee	11 L/3&4D	23°41′59.37″N, 86°25′57.13″E
B-V (A&B)	Salanpur	–	23°48′29.78″N, 86°17′52.67″E

[a] R = Raniganj Formation; B = Barakar Formation

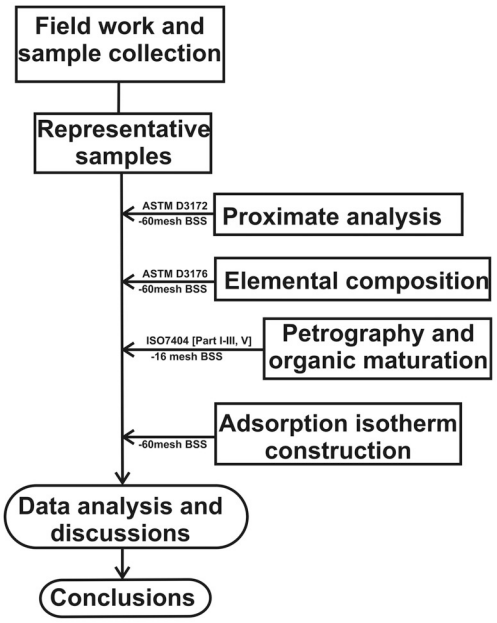

Fig. 3. Methodology followed in the present investigation.

elemental analyzer to determine the elemental C, H, N, S and O (by difference) following standard ASTM D3176 (1979).

3.3. Petrographic study

For petrographic analyses, samples were crushed to −16 BSS mesh size (ISO 7404-2, 1985). Pellets were prepared in 1″ cube size molds using carnauba wax and left overnight at room temperature for hardening. The sample pellets were polished to provide clear vision of coal grains under microscope for quality analyses. The maceral analysis was carried out as per the standard ISO 7404-3, ISO (1994) and random reflectance as per the standard ISO 7404-5 (1994) using Leica make DM 4500P microscope with MSP attachment. The maceral and reflectance analyses were carried out under 50× oil immersion objective and liptinite macerals were identified with fluorescence light.

3.4. Adsorption isotherm experiment

Approximately, 500 g of samples were separated by coning and quartering for adsorption experiments. The samples were prepared in −0.25 mm or 60 BSS mesh grain size to investigate the adsorption capacity of all the samples at 30 °C. ASTM standard was followed for determination of the equilibrium moisture of the coals at 96 to 97% relative humidity (RH) at 30 °C (ASTM D1412/D1412M, 2015). Adsorption isotherm experiment involves mainly two steps i.e. Measurement of dead/void volume within the experimental setup and determination of adsorption capacity. After the dead volume is determined, the entire setup was evacuated again for adsorption isotherm construction. Methane was added to the reference cell and allowed to equilibrate at the bath temperature before admitting to sample cell. The sample cell was then connected to reference cell and allowed to equilibrate. The drop in pressure so caused was corrected for void volume to calculate the actual amount of gas adsorbed in coal. The procedure is repeated at incremental pressure steps of about 1.0 MPa until the desired pressure of 12 MPa was achieved for all the samples. The volume of gas adsorbed at each pressure step was used to construct the adsorption isotherm. The total amount of adsorption was calculated using the following equation:

$$n_{adsorbed} = n_{injected} - n_{unadsorbed}$$

where,

$$n_{injected} = \left(\frac{PV}{Z_{methane}RT}\right)reference \text{ and } n_{unabsorbed} = \left(\frac{PV_{void}}{Z_{methane}RT}\right)sample.$$

Volume of gas adsorbed by this process does not take into account the gas adsorbed into the pore spaces of the adsorbent that is known as excess sorption or Gibbs sorption. Though excess sorption is insignificant at low pressures, the absolute values may be substantially different from excess sorption at higher pressures (Arri et al., 1992; Hall et al., 1994; Mohanty, 2019) and were calculated using the following equation:

Table 2
Results of proximate and ultimate analyses of coals from Raniganj Formation, Raniganj Sub-basin and Barakar Formation, Jharia Sub-basin.

Sample ID	Proximate Analyses, *wt%*				Ultimate Analyses, *wt%*					Atomic Ratios	
	A	M	VM[a]	FC[a]	C[a]	H[a]	N[a]	S[a]	O[a]	H/C	O/C
Raniganj formation / Raniganj sub-basin											
R-X (A)	16.8	4.6	39.5	60.5	79.2	4.3	2.3	0.4	13.8	0.65	0.13
R-X (B)	16.4	4.5	39.6	60.4	80.6	4.5	2.3	0.3	12.3	0.67	0.11
R-VIII (A)	14.7	3.4	40.2	59.8	82.8	5.6	2.8	0.7	8.1	0.81	0.07
R-VIII (B)	14.3	3.3	40.2	59.8	82.0	5.5	2.4	0.5	9.6	0.80	0.09
R-VI (A)	27.0	3.6	38.8	61.2	84.8	4.8	2.9	0.4	7.1	0.68	0.06
R-VI (B)	27.2	3.6	39.2	60.8	81.4	5.4	3.9	0.6	8.7	0.80	0.08
R-IV (A)	10.0	2.6	39.0	61.0	83.7	5.5	3.8	0.3	6.7	0.79	0.06
R-IV (B)	10.1	2.6	39.3	60.7	83.1	5.3	4.0	0.3	7.3	0.77	0.07
R-III (A)	15.1	2.5	39.1	60.9	84.1	5.5	3.6	0.4	6.4	0.78	0.06
R-III (B)	15.8	2.7	39.1	60.9	85.4	5.4	3.4	0.5	5.3	0.76	0.05
Barakar formation /Jharia sub-basin											
B-XI (A)	17.0	0.9	21.8	78.2	86.7	3.8	2.0	0.5	7.0	0.53	0.06
B-XI (B)	16.7	0.9	21.8	78.2	85.6	3.7	2.0	0.4	8.3	0.52	0.07
B-IX (A)	27.0	0.6	21.5	78.5	90.9	3.9	2.0	0.6	2.6	0.51	0.02
B-IX (B)	26.9	0.5	21.3	78.7	91.9	4.1	2.3	0.6	1.1	0.54	0.01
B-VIII (A)	24.0	0.6	21.0	79.0	89.5	4.0	1.9	0.7	3.9	0.54	0.03
B-VIII (B)	23.8	0.7	20.8	79.2	92.0	3.9	2.0	0.6	1.5	0.51	0.01
B-VII (A)	27.8	0.7	21.9	78.1	90.8	4.3	1.9	0.5	2.5	0.57	0.02
B-VII (B)	27.4	0.8	22.0	78.0	89.4	5.4	2.3	0.5	2.4	0.72	0.02
B-V (A)	32.9	1.0	20.9	79.1	91.3	4.2	2.0	0.7	1.8	0.55	0.01
B-V (B)	32.9	1.1	20.7	79.3	90.9	4.3	2.0	0.9	1.9	0.57	0.02

[a] Values are in dry mineral matter free basis.

Table 3
Results of petrographic analysis of coals from Raniganj Formation, Raniganj Sub-basin and Barakar Formation, Jharia Sub-basin.

Sample ID Raniganj	Maceral[a], %				V-step distribution					% R_r
	V	I	L	MM						
R-X (A)	69.3 (71.6)	18.9 (19.5)	8.6 (8.9)	3.2	V_4 24	V_5 68	V_6 8			0.53
R-X (B)	68.3 (70.3)	18.9 (19.4)	10.0 (10.3)	2.8	V_4 30	V_5 72	V_6 6	V_7 2		0.53
R-VIII (A)	71.1 (73.6)	17.3 (17.9)	8.2 (8.5)	3.4	V_5 70	V_6 30				0.58
R-VIII (B)	71.2 (73.8)	16.2 (16.8)	9.1 (9.4)	3.5	V_4 3	V_5 92	V_6 19			0.56
R-VI (A)	66.3 (69.4)	15.3 (16.0)	14.0 (14.6)	4.4	V_5 3	V_6 94	V_7 3			0.65
R-VI (B)	68.0 (71.7)	14.9 (15.7)	12.0 (12.6)	5.1	V_5 4	V_6 116	V_7 5			0.65
R-IV (A)	77.0 (79.1)	14.4 (14.8)	5.9 (6.1)	2.7	V_6 65	V_7 34	V_8 1			0.69
R-IV (B)	78.1 (80.1)	13.5 (13.9)	5.8 (6.0)	2.6	V_5 1	V_6 61	V_7 32	V_8 1		0.68
R-III (A)	74.3 (78.1)	11.3 (11.9)	9.5 (10.0)	4.9	V_5 2	V_6 42	V_7 52	V_8 4		0.71
R-III (B)	74.1 (78.0)	12.5 (13.1)	8.5 (8.9)	4.9	V_6 55	V_7 75	V_8 9			0.72
Jharia										
B-XI (A)	71.3 (75.1)	19.8 (20.8)	3.9 (4.1)	5.0	V_{10} 7	V_{11} 38	V_{12} 46	V_{13} 9		1.21
B-XI (B)	73.1 (76.5)	18.1 (19.0)	4.3 (4.5)	4.5	V_{10} 5	V_{11} 32	V_{12} 65	V_{13} 7	V_{14} 1	1.22
B-IX (A)	73.4 (78.2)	15.9 (16.9)	4.6 (4.9)	6.1	V_{10} 15	V_{11} 33	V_{12} 40	V_{13} 12		1.20
B-IX (B)	75.1 (79.7)	14.9 (15.8)	4.2 (4.5)	5.8	V_{10} 9	V_{11} 29	V_{12} 56	V_{13} 12		1.22
B-VIII (A)	66.4 (70.4)	22.4 (23.7)	5.6 (5.9)	5.6	V_{10} 8	V_{11} 30	V_{12} 40	V_{13} 19	V_{14} 3	1.23
B-VIII (B)	68.5 (72.3)	20.9 (22.0)	5.4 (5.7)	5.2	V_{10} 13	V_{11} 55	V_{12} 69	V_{13} 11	V_{14} 1	1.20
B-VII (A)	70.3 (75.8)	17.2 (18.5)	5.3 (5.7)	7.2	V_9 7	V_{10} 27	V_{11} 44	V_{12} 16	V_{13} 6	1.14
B-VII (B)	70.7 (75.9)	17.0 (18.2)	5.5 (5.9)	6.8	V_9 5	V_{10} 43	V_{11} 84	V_{12} 46	V_{13} 20	1.17
B-V (A)	67.3 (72.5)	16.6 (17.9)	8.9 (9.6)	7.2	V_{10}	V_{11} 32	V_{12} 13			1.09
B-V (B)	66.3 (71.6)	18.4 (19.9)	7.9 (8.5)	7.4	V_8 5	V_9 17	V_{10} 55	V_{11} 32	V_{12} 11	1.11

V: Vitrinite, I: Inertinite, L: Liptinite, MM: Mineral Matter, R_r: Random Reflectance.
[a] Values in the parenthesis are on mineral matter free basis.

$$N_{absolute} = n_{excess}/(1 - [\rho_{gas}/\rho_{adsorbed}])$$

where, N or n, no. of moles; P, pressure; V, volume; R, universal gas constant; T, temperature; ρ, density and Z, compressibility factor.

The rate of gas sorption decreases with increasing pressure eventually reaching a maximum value of sorbed gas which denoted as Langmuir volume (V_L) and the pressure at which gas sorption capacity equals one half of the maximum value ($V_L/2$) represents Langmuir pressure (P_L). Langmuir parameters are calculated from the model fit for adsorption isotherm data.

4. Results

4.1. Chemical composition

The results of proximate and ultimate analyses of Raniganj coals from Raniganj Sub-basin and Barakar coals from Jharia Sub-basin are presented in Table 2. The moisture content varies in two distinct ranges being comparatively higher for Raniganj coal (2.5–4.6%, air-dried basis) than the Barakar coals (0.5–1.1%, air-dried basis). The ash content is significantly low in Raniganj formation coal (Table 2), mostly ranging between 10.0 and 16.8% (air-dried basis) except R-VI seam coal (~27%, air-dried basis). The ash content of the Barakar coals from the Jharia Sub-basin varies widely in between 16.7 and 32.9% (air-dried basis) and typically higher than the Raniganj coals. The volatile matter content for both the coals varies within a narrow range and, distinctly different for the set of coals being higher for the Raniganj coals (38.8–40.2%, dmmf basis) and lower for the Barakar coals (20.7–22.0%, dmmf basis).

Like the proximate analyses results, the elemental compositions for the two sets of coals are very distinctive from each other. Overall carbon content (Table 2) of the studied sample varies within the range 79.2–92.0% (dmmf basis) and nitrogen content between 1.9 and 4.0% (dmmf basis) for both the coals. The oxygen content of these coals varies between 1.1 and 13.8% (dmmf basis). However, sulfur content of both the coals is very less and varies between 0.3 and 0.9% (dmmf basis). The carbon content for the Raniganj coals of Raniganj Sub-basin and Barakar coals of Jharia Sub-basin is 79.2–85.4% (dmmf basis) and 85.6–92.0% (dmmf basis), respectively and the hydrogen content is 4.3–5.6% and 3.7–5.0%, respectively. The nitrogen content vary within a very narrow yet distinct ranges for the Raniganj coals (2.3–4.0%, dmmf basis) of Raniganj Sub-basin and Barakar coals (1.9–2.3%, dmmf basis) of Jharia Sub-basin and sulfur content is 0.3–0.7% and 0.4–0.9%, respectively.

4.2. Petrography

The maceral composition and random reflectance (R_r) values determined through petrographic analyses are presented in Table 3. Overall range of random reflectance value of the suite of coals is 0.53–1.23%. The Raniganj coals (0.53–0.72%) of Raniganj Sub-basin have lower reflectance than the Barakar coals (1.09–1.23%) of Jharia Sub-basin. The B-VIII seam coal from Jharia shows the highest reflectance value of 1.23%. The lower reflectance values of Raniganj coals (0.53–0.72%) of Raniganj Sub-basin (Table 3) compared to the Barakar coals of Jharia Sub-basin indicate that these coals are less mature and have evolved through a different kind of thermal history than that of Jharia sub-basin.

Indian coals are highly intermixing in terms of the maceral association (Choudhury et al., 2008). The organic precursor and depositional condition can be assessed from maceral composition. The coals from both the formations, Raniganj (69.4–80.1%, mmf basis) and Barakar (70.4–79.7%, mmf basis), are dominated by vitrinite group macerals (Table 3). The inertinite content of the Barakar coals of Jharia ranges between 15.8 and 23.7% (mmf basis) compared to 11.9–19.5% (mmf basis) in Raniganj coals of Raniganj, which indicate formation of Jharia coals in an oxygen rich depositional environment. The Raniganj coals of Raniganj Sub-basin are rich in liptinite (6.0–14.6%, mmf basis) compared to Barakar coals of Jharia Sub-basin (4.1–9.6%, mmf basis), and may be attributed to the lesser maturity and different precursor materials of the former coals. Such variation indicates that the Jharia coals are more mature and have approached the peak for thermogenic methane generation. These coals are mostly having sporinite with few resinites and bituminites among the liptinite group macerals. The visible mineral matter observed during petrographic analyses lies mostly between 2.6 and 4.9% for the Raniganj coals and 4.5–7.2% for the Jharia coals which corroborates the ash content found from the proximate analysis. The mineralogy of these coals is dominated by clay minerals with some silicates and carbonates. The mineral content in the Barakar coals of Jharia Sub-basin is higher and decreases upward indicating lesser influx of detritus material associated with low rate of basin subsidence. The maceral distributions are presented in Fig. 4.

Collotelinite and collodetrinite macerals of vitrinite group are common in the Raniganj and Barakar coals. Among the liptinite maceral group, thin walled sporinites are found frequently in association with vitrinites in Raniganj coals. Along with the sporinite, cutinite is also found embedded in collotelinites of these coals (Fig. 5c) in addition

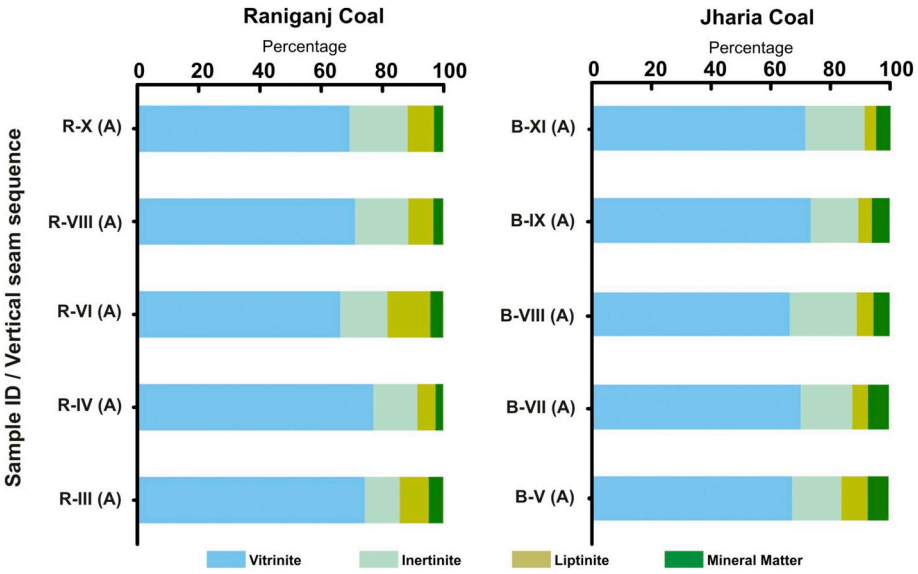

Fig. 4. Petrographic composition for the studied *(a)* Raniganj Formation coals from Raniganj Sub-basin *(b)* Barakar Formation coals from Jharia Sub-basin.

to small amount of bitumen (Mohanty et al., 2018). Slightly lower reflectance value for B—V seam than the overlying seams may be due to the sample being collected from mine that flanked the synclinal basin with lesser depth of burial. On the other hand, the samples of B-VIII, B-IX and B-XI were located towards the basin depocentre with higher depth of burials. Further, some heat effected vitrinite grains are also observed in B-VIII seam coal from Jharia Sub-basin (Fig. 6b). This indicates the local influence of intrusive, mostly mica-peridotites (Michalski et al., 1997), on the studied coal samples that explains the slightly enhanced reflectance values for the central coal seams. Among inertinite group, fusinite, semifusnite and inertodetrinite are the commonly found macerals in these coals. However, fusinite content is higher for Barakar coals of Jharia Sub-basin. The precursors of inertinite are mainly the same as those for vitrinites, namely cellulose and lignin from the cell walls of plants with relatively high carbon contents, low hydrogen contents and a much increased level of aromatization. The development of high inertinite contents in Barakar coals of Jharia Sub-basin may be attributed to their formation under relatively dry depositional conditions, or as the result of alternating high and low groundwater tables, due to intermittent drainage of the peat surface (Stach, 1982). Some of the semifusinites are showing honeycomb structure with thick cell walls. Broken bogen structure in fusinites was found in both Raniganj and Barakar formation coals. Liptodetrinite in groundmass of detrovitrinite (Fig. 6b) are found in B-VIII seam coal of Jharia Sub-basin. Some carbonate minerals within vitrinite were observed in both the coals (Fig. 6c).

4.3. Adsorption isotherm construction

The high pressure methane adsorption isotherm experiments on the moisture-equilibrated coals (96–97% RH at 30 °C) were performed at 30 °C up to a maximum pressure of 12 MPa. Experimental results fitted to the Langmuir equation and the regression coefficients (R) are shown in Table 4. Langmuir volume (V_L) and Langmuir pressure (P_L) were recalculated for dry ash-free (daf) basis. The Langmuir volume ranges from 9.3 to 21.8 cc/g (daf basis) for Raniganj coals and 21.1–29.1 cc/g (daf basis) for Jharia coals. The Langmuir pressure ranges between 1316 and 2998 KPa for Raniganj coals of Raniganj Sub-basin and 1355–3420 KPa for Barakar coals of Jharia Sub-basin. The isotherms constructed for both the coals on as received basis and Langmuir model fit curves are shown in Figs. 7 & 8. The Langmuir volume is highest for seam R-IV seam and lowest for uppermost R-X seam among the Raniganj coals. Langmuir volume is higher for Barakar coals than the Raniganj coals and among the Barakar coals it is highest in seam B-IX and lowest in seam B—V (daf basis). The Barakar coals of Jharia Sub-basin show comparatively higher adsorption capacity than the Raniganj coals of Raniganj Sub-basin.

5. Data analysis and discussion

Gondwana sedimentation commenced with the deposition of glacial sediments. With the retreat of glaciers at the close of glacial epoch, the irregular topography of the Indian Peninsula was filled by the swamps rich in vegetal matter. The conditions were favourable for deposition of coaliferous sediments of early Permian Barakar Formation. After the deposition of the coal bearing sediments, a thick sequence of ironstone shales were deposited in Damodar Valley in closed basins under reducing environments favourable for precipitation of the iron carbonates and is known as Barren Measures. The coal forming conditions were again prevalent during the deposition of late Permian Raniganj Formation. The Permian coal in the Damodar valley is the resultant of basin burial and upliftment. The present day geothermal gradients of Damodar Valley basins vary between 31 °C/km to 57 °C/km (Casshyap and Tewari, 1987). During Permian time a tensional tectonic regime probably existed in India centered in the Jharia Basin resulting in extensive subsidence and, consequently, a thicker sedimentary sequence of about 2.5–3.5 km was deposited in the Jharia Basin than in any other Gondwana basins of India. The Jharia sub-basin occurred under a much higher geothermal gradient during the Permian and possibly the Triassic (Kraiser et al., 1964). Patel et al. (2014) showed that the maximum pre-depositional temperature is about 110–120 °C in the Raniganj Sub-basin. The sub-basins of the Damodar Valley were further impacted by igneous activity during the Cretaceous, associated with the Rajmahal flood basalt magmatism of the Eastern Indian Shield, which resulted in an intensive swarm of dolerite dykes penetrating the Permian Formations (Srivastava et al., 2009). This is apparent from the Barakar coals of the Jharia Sub-basin having higher reflectance value, higher carbon content, less moisture, less VM compared to the Raniganj coals of the Raniganj Sub-basin (Fig. 9).

Elemental carbon composition shows difference in thermal maturity between the younger Raniganj Formation coals of Raniganj Sub-basin and older Barakar Formation coals of Jharia Sub-basin. A clear indication of the second coalification jump for Barakar coals of Jharia is observed as most of the coals have carbon content > 87% on dmmf basis, some (B—V, B-VIII, B-IX) even approaching towards third coalification jump. As per ASTM D388 (2018) classification of coal rank,

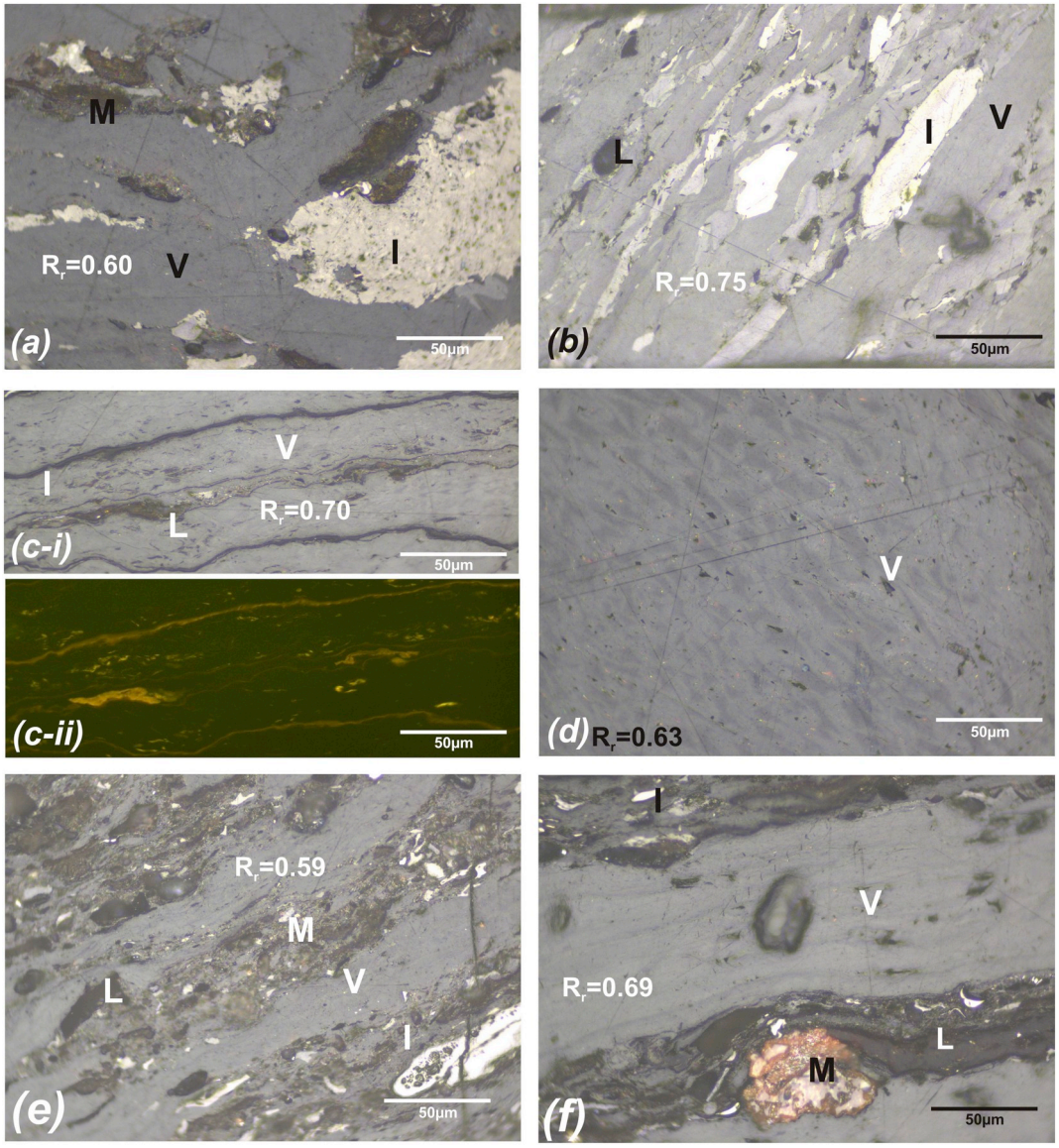

Fig. 5. Photomicrographs showing *(a)* fusinite and mineral matter associated with collotellinite *(b)* fusinite and inertodetrinite embedded in collotelinite *(c-i)* tenuicutinite embedded in telinite *(c-ii) c-i*, under fluorescence light *(d)* telovitrinite *(e)* liptodetrinite, inertodetrinite and mineral matter in collotelinite *(f)* carbonates within liptinite band associated with alternate bands of collotelinite found in coal seams of Raniganj Formation, Raniganj Sub-basin. 50× oil immersion objective. V, vitrinite; I, inertinite; L, liptinite; M, mineral matter. Random reflectance (R_r) values of respective grains are mentioned on the photomicrographs.

chemical analyses data of the studied reveals that Raniganj coals of Raniganj Sub-basin belong to high volatile bituminous A type whereas the Barakar coals of Jharia Sub-basin belong to medium volatile bituminous to low volatile bituminous type.

5.1. Gas generation potential: organic matter type and maturation

The compositional changes are indicative of the maturity stage of a particular kerogen and include loss of hydrogen, oxygen, nitrogen, and sulfur in the form of different functional groups that further promote aromatization associated with increasing depth of burial. Various gases are evolved during thermal transformation of organic matter during coalification. CO_2 and CH_4 are the principal gases formed at low and high rank, respectively. Deoxygenation reactions including decarboxylation and dehydroxylation primarily occur in low rank coals below 85% C and after this rank, dehydrogenation reactions set in. Aromatization leads to proper molecular stacking in sheets thereby increase in molecular density and vitrinite reflectance, as well as changes in spore coloration, with increasing depth. The microporosity increases with increase in aromaticity which in turn increases the sorption capacity of the coals with increase in rank.

Type of organic matter and thermal maturity of a source rock determines its hydrocarbon generation potential. Elemental compositions are taken as atomic ratios and plotted in van Krevelen diagram (Van Krevelen, 1993). Due to kerogen mixtures, however, obtaining maturity only through elemental analyses is approximate (Tissot and Welte, 1984). Hence, vitrinite reflectance is the most reliable and commonly used maturity parameter measured on the rock and kerogen (Hunt, 1996). Based on the vitrinite reflectance and other maturity parameters source rocks are identified as immature, mature and over mature rock (Fig. 10). The early biogenic gas generation starts below vitrinite reflectance value of < 0.5% and is not significant for generating hydrocarbons (Cornford, 1998). Significant methane generation is mainly due to thermal origin and occurs at high-volatile bituminous and higher ranks having the vitrinite reflectance value > 0.6% (Rice, 1993).Thermally mature source rocks are exposed to the temperature range of 50 °C–200 °C having the vitrinite reflectance value ranging between 0.5 and 1.35% (Peters and Cassa, 1994). With the increase of burial depth

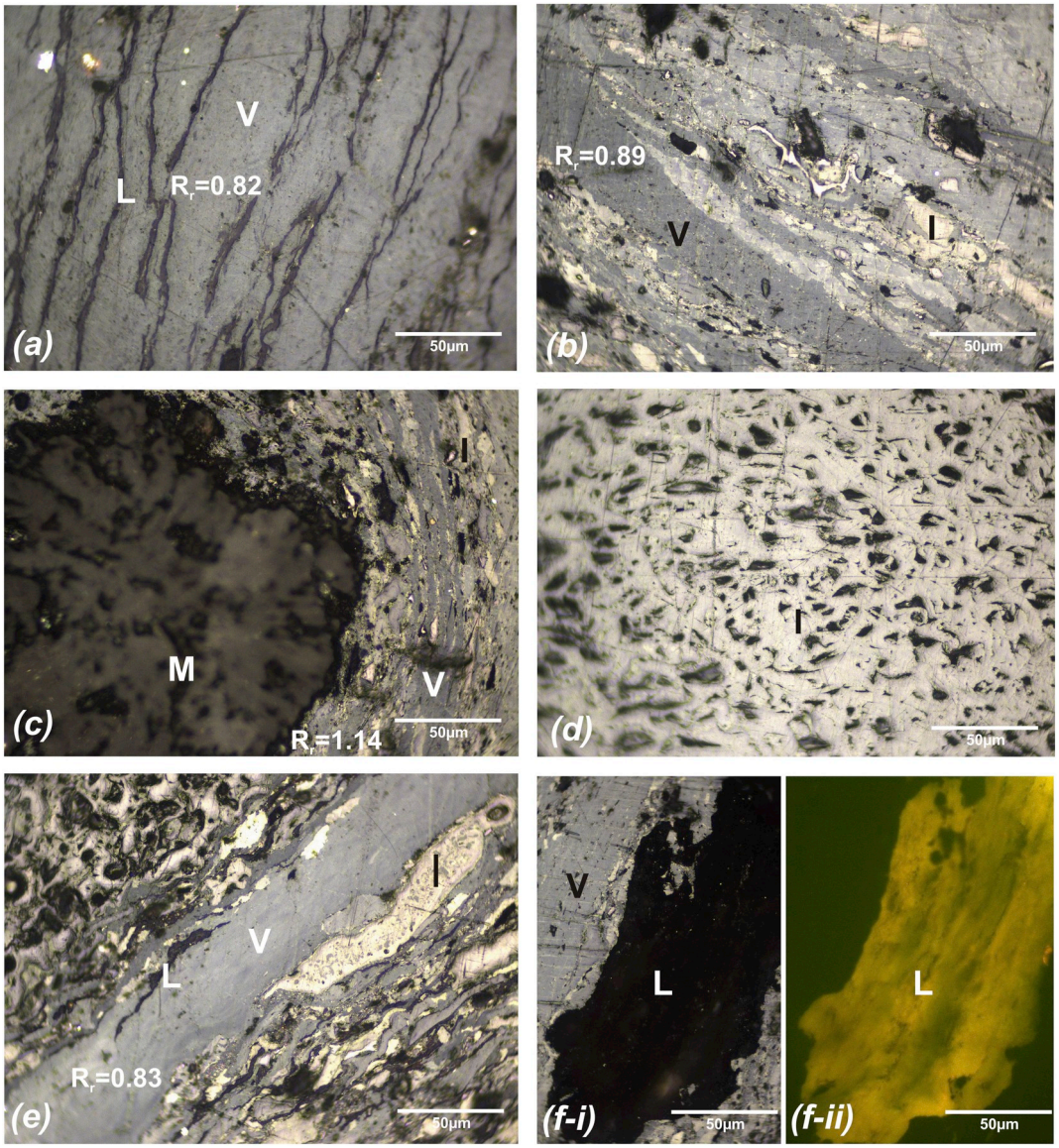

Fig. 6. Photomicrographs showing *(a)* collotelinite with tenuicutinites *(b)* trimacerities with alternate bands of collotelinite and semifusinite *(c)* carbonate mineral associated with vitrinite *(d)* fusinite grain *(e)* trimaceraites with collotelinite band *(f-i)* resinite in association with collotelinite and inertodetrinite *(f-ii) f-i*, under fluorescence light found in coal seams of Barakar Formation, Jharia Sub-basin. 50× oil immersion objective. V-vitrinite; L-liptinite; I-inertinite; M-Mineral Matter. Random reflectance (R_r) values of respective grains are mentioned on the photomicrographs.

and temperature, pressure also increases considerably, beyond the diagenesis stage. The Barakar coals of the Jharia Sub-basin, however, show distinctly higher maturity (0.81–1.23%) than the Raniganj coals of the Raniganj Sub-basin with peak hydrocarbon generation potential. Potential CBM generating coals have reflectance values between 0.7 and 2.0% (Chandra, 1997).

The van Krevelen diagram is used to distinguish the kerogen type and maturity to have an idea about the source rock for gas generation from the coals of Barakar and Raniganj Formations using the atomic ratios H/C vs O/C. The van Krevelen diagram shows the trend of elimination of CO_2, water and other volatile constituents, and generation of methane from different kerogens during coalification (Tissot et al., 1974). The Barakar coals of the Jharia Sub-basin show significantly higher maturity than the Raniganj coals of Raniganj Sub-basin in terms of atomic ratios while plotted on van Krevelen diagram (Fig. 11a). The hydrogen content is a measure of kerogen type. Kerogen having H/C ratios > 1.2 are oil prone and while the ratios mainly range between 0.50 and 0.80, tend to generate mostly gas (Walters, 2006). H/C atomic ratio of the studied Raniganj and Barakar coals varies between 0.65 and 0.80 and 0.51–0.72 i.e., lying within the range of 0.51–0.80 and is prone to gas generation. The O/C atomic ratio varies between 0.05 and 0.13 and 0.01–0.07, respectively (Table 2). Both the atomic ratios of the studied coals show an overall decreasing trend with the vitrinite reflectance value, depicting the loss of hydrogen and oxygen with increase in maturity.

Kerogen Type I and II are oil-prone, Type III is gas-prone, and Type IV is inert carbon. Most of the studied coals of Raniganj Formation of Raniganj Sub-basin fall in between the Type-III kerogen type whereas those of Barakar Formation of Jharia Sub-basin falls within kerogen Type-III and few tend towards Type-IV, and belong to oil-prone zone and gas prone zone, respectively. The Raniganj coals of Raniganj Sub-basin have achieved wet gas maturity stage approaching early-thermogenic methane generation whereas Barakar coals of Jharia Sub-basin reached condensate gas stage approaching peak-thermogenic methane generation (Fig. 10). The ternary plot for the maceral distribution shows that all the coals from Raniganj and Barakar Formations lies within Type-III kerogen (Fig. 11b). The Raniganj coals of Raniganj Sub-basin are rich in liptinites than the Barakar coals of Jharia Sub-basin

Table 4
Results of adsorption isotherm construction for coals Raniganj Formation, Raniganj Sub-basin and Barakar Formation, Jharia Sub-basin.

Sample ID	Langmuir Volume (V_L, cc/g)		Langmuir pressure (P_L, KPa)	Regression coefficient (R)
	as received (ar)	dry ash free (daf)		
Raniganj formation / Raniganj sub-basin				
R-X (A)	7.2	9.3	1316	0.9989
R-X (B)	7.9	10.2	1571	0.9270
R-VIII (A)	12.8	15.7	2998	0.9978
R-VIII (B)	12.0	14.6	2639	0.9672
R-VI (A)	7.6	11.1	1317	0.9921
R-VI (B)	9.6	14.1	2620	0.9671
R-IV (A)	19.5	21.8	2599	0.9980
R-IV (B)	17.9	20.1	2371	0.9611
R-III (A)	15.3	18.4	2305	0.9996
R-III (B)	15.6	19.0	2349	0.9606
Barakar formation /Jharia sub-basin				
B-XI (A)	19.9	24.3	1355	0.9998
B-XI (B)	21.1	25.7	1641	0.9328
B-IX (A)	21.0	29.1	3420	0.9995
B-IX (B)	19.9	27.6	3244	0.9773
B-VIII (A)	16.3	21.6	1559	0.9998
B-VIII (B)	17.3	22.9	1676	0.9345
B-VII (A)	18.5	26.2	3235	0.9992
B-VII (B)	18.1	25.4	3067	0.9750
B-V (A)	13.9	21.1	2210	0.9998
B-V (B)	14.6	22.1	2073	0.9521

and they have two different levels of maturity. The decrease in volatile matter content of the Barakar coals of Jharia Sub-basin is attributed to the second stage of coalification jump (with volatile matter < 27%).

Bandopadhyay and Mohanty (2014) while investigating the vitrinite concentrates from Indian coals of varying rank inferred that the evolution in maturity in the bituminous range takes place in two distinct but contiguous stages as indicated by the change in slope at $R_r \approx 0.80–0.90$ (C ≈ 85%) in the plots C vs. R_r and O vs. R_r (Fig. 12 a, b) representing a change in the dominant geochemical processes at different stages. This also refers to the 2nd stage of coalification jump (Larsen et al., 1986). The relationship between the two important rank parameters i.e. vitrinite reflectance and carbon contents for Raniganj coals of Raniganj Sub-basin and Barakar coals of Jharia Sub-basin is shown in Fig. 12(a) along with the data points for Indian vitrinites as established by Bandopadhyay and Mohanty (2014). Overall a strong positive relationship is observed between vitrinite reflectance and carbon. Similar relationships has also found for the British Carboniferous coals by Chandra (1962) and different Indian coals belonging to different geological ages by Chandra and Chakrabarti (1989) and low rank vitrinites of Carboniferous coals of Central Massif, France by Jiménez et al. (1999). The relationship between vitrinite reflectance and oxygen content is plotted in Fig. 12(b), shows an overall decreasing trend. Hence, it may be inferred that the Raniganj coals of Raniganj Sub-basin and Barakar coals of Jharia Sub-basin belong to two distinct stages of coalification and, the sub-basins were subjected to different basinal and thermal history.

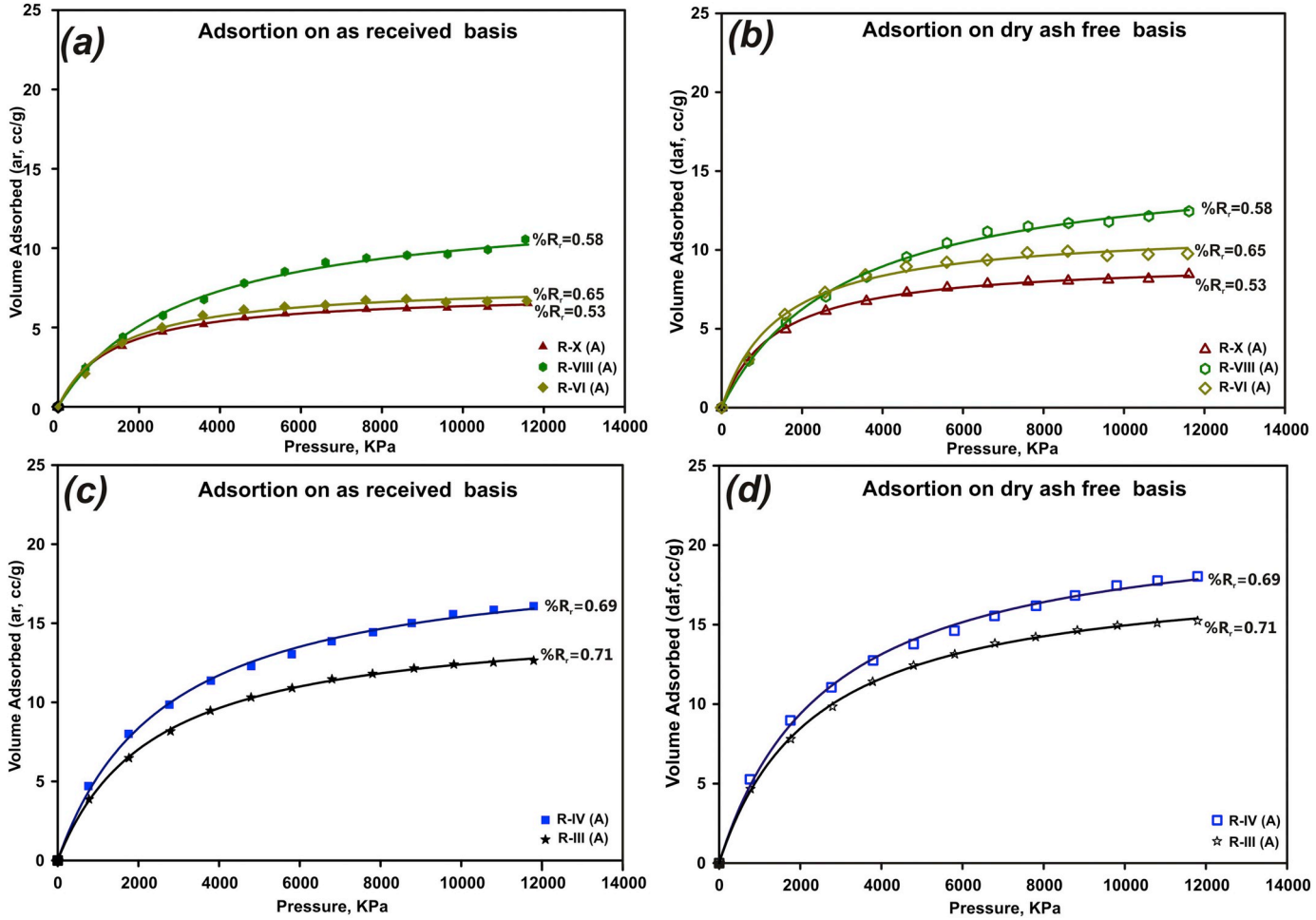

Fig. 7. Methane adsorption isotherm constructions of *(a)* R-X (A), R-VIII (A), R-VI (A) samples *(b) a*-daf basis *(c)* R-IV (A) and R-III (A) samples *(d) c*-daf basis for coal seams of Raniganj Formation, Raniganj Sub-basin.

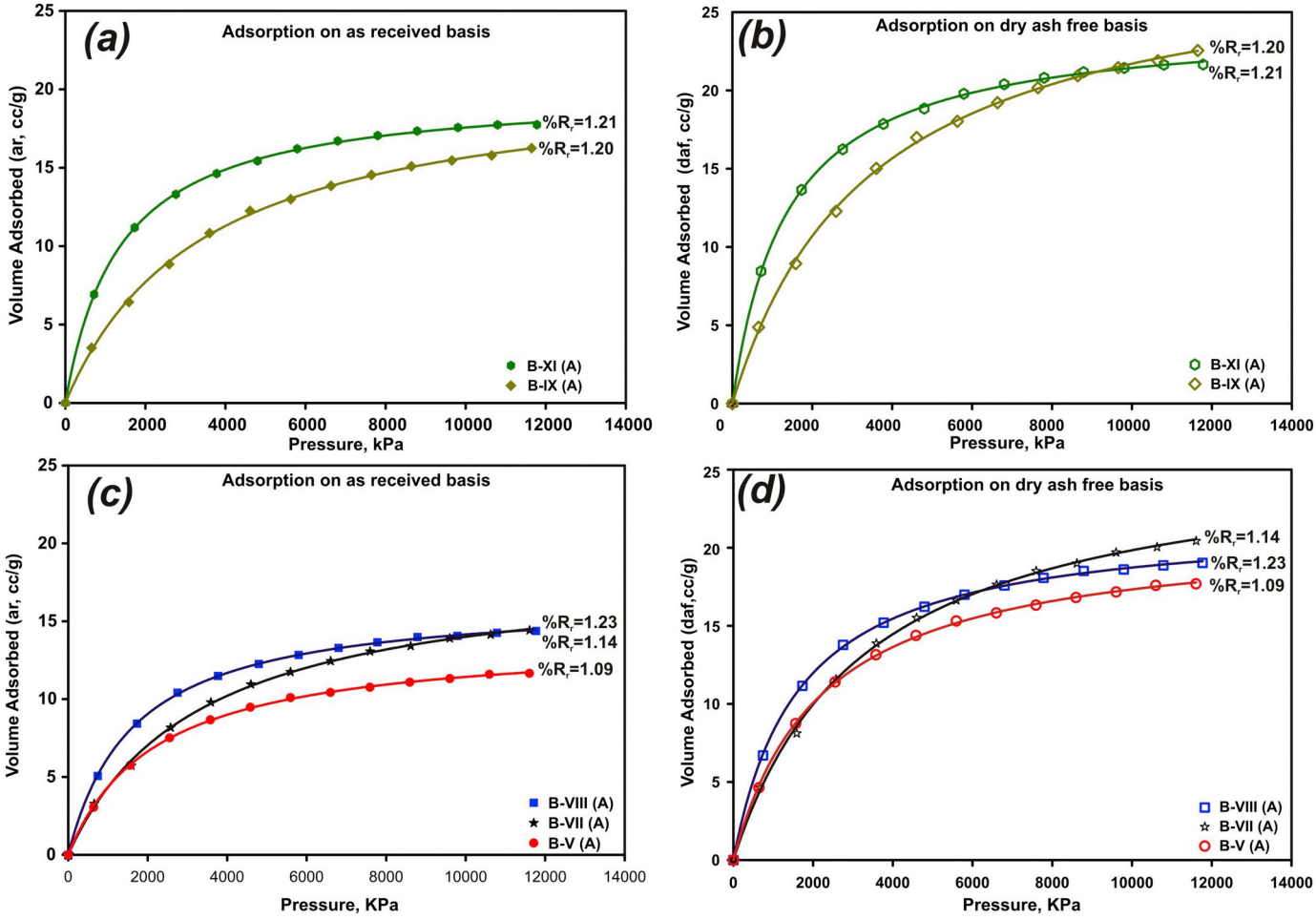

Fig. 8. Methane adsorption isotherm constructions of *(a)* B-XI (A), B-IX (A) *(b) a*-daf basis *(c)* B-VIII (A), B-VII (A), B−V (A) *(d) c*-daf basis for coal seams of Barakar Formation, Jharia Sub-basin.

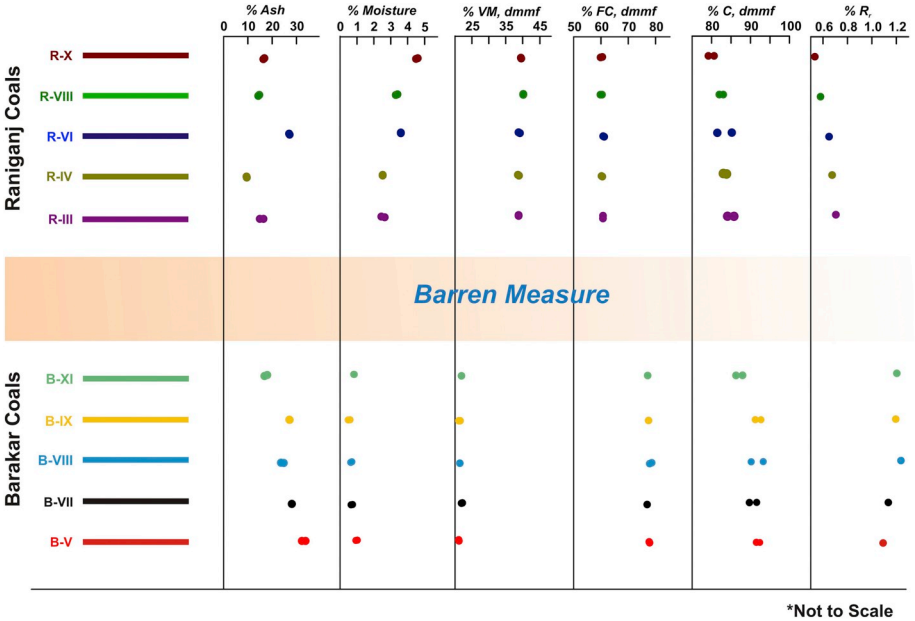

Fig. 9. Variation in chemical and rank parameters along the stratigraphic column for the coals of Raniganj Formation, Raniganj Sub-basin and Barakar Formation, Jharia Sub-basin.

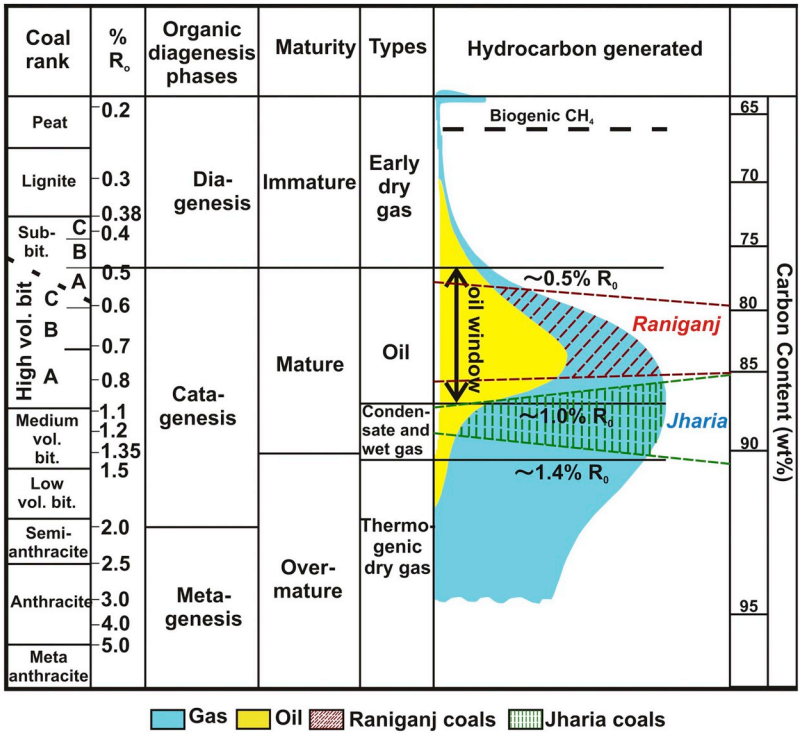

Fig. 10. Schematic diagram of coal maturity with hydrocarbon generation potential with different shades for data on coals from Raniganj Formation, Raniganj Sub-basin and Barakar Formation, Jharia Sub-basin (modified after Juntgen and Karweil, 1966).

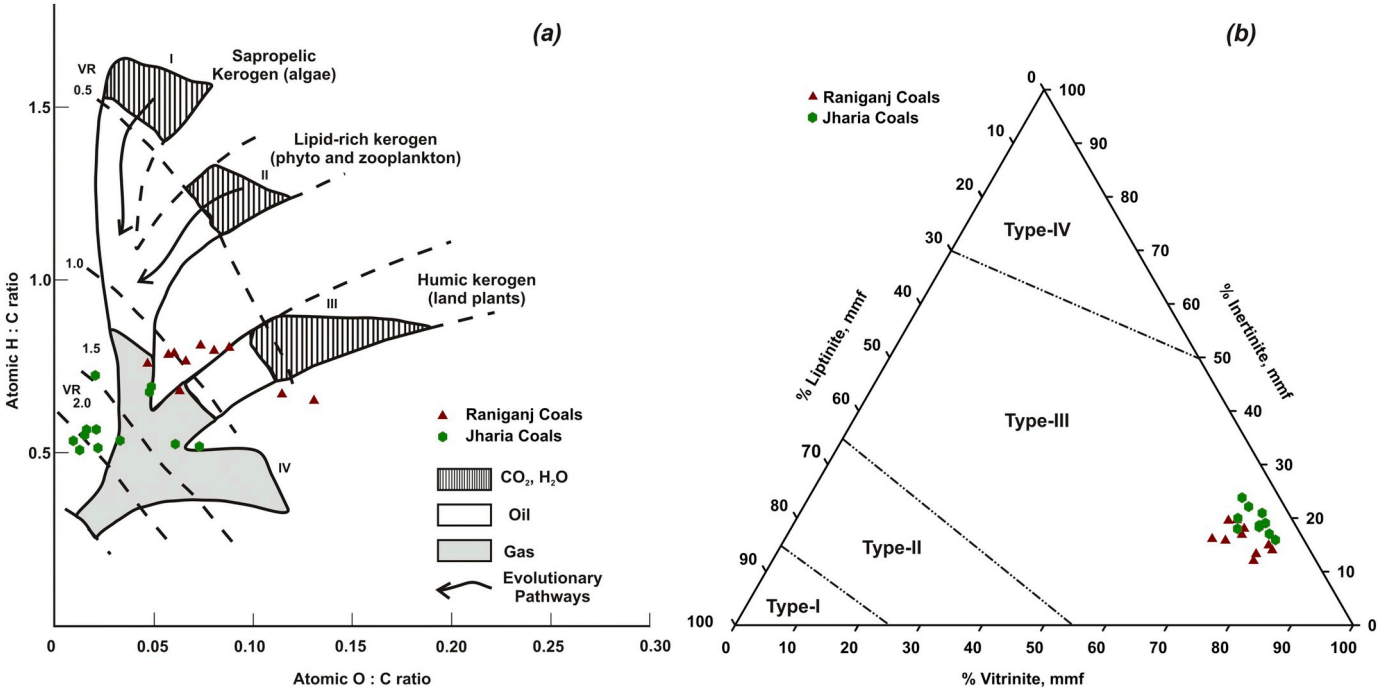

Fig. 11. (a) van Krevelen diagram for kerogen type (b) Ternary plot for maceral distribution (adapted from Cornford, 1998; Togunwa et al., 2015) for the coals of Raniganj Formation, Raniganj Sub-basin and Barakar Formation, Jharia Sub-basin.

5.2. Effect of moisture on methane adsorption capacity

The multiple regression analysis was carried out to evaluate the main effects as well as interaction effects of the variables. Prior to that simple regression analysis was performed to observe the dependency relationship between the parameters (Hogg et al., 2005). For each plot, *P*-value (probability) has been determined and the 95% confidence interval limit is shown in Fig. 13–16 to assess the statistical significance of the observed relationship between the variables. The effects of moisture on methane adsorption capacity by coal are well documented (Joubert et al., 1974; Yalçin and Durucan, 1991; Levine, 1993; Crosdale et al., 2008). The plot between Langmuir volume (V_L) and moisture content (M) is shown in Fig. 13(a). Both the parameters have been taken in as received basis for comparison. Although the moisture

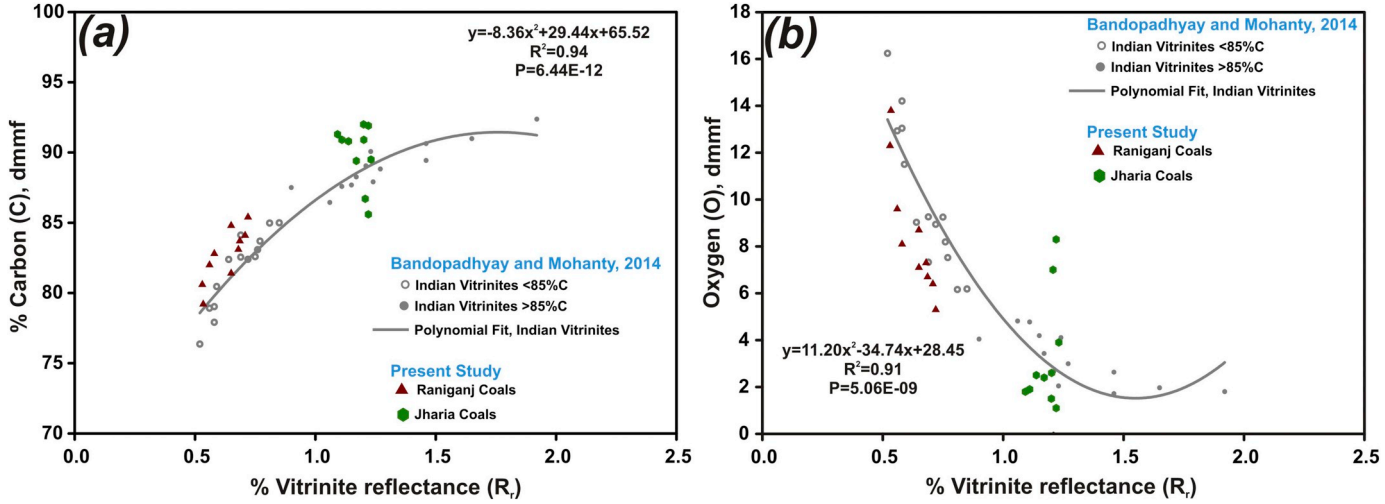

Fig. 12. Relationship of reflectance with *(a)* carbon (dmmf), *(b)* oxygen (dmmf) for the coals of Raniganj Formation, Raniganj Sub-basin and Barakar Formation, Jharia Sub-basin (data for Indian vitrinites were adapted from Bandopadhyay and Mohanty (2014).

content is completely distinct for two sets of separate coals from Raniganj and Jharia Sub-basins, it shows an overall decreasing trend with the adsorption capacity. The relationship is weaker for Jharia coals ($R^2 = 0.24$, linear) and is statistically insignificant as $P > 0.05$, whereas the regression coefficient is significantly high for the Raniganj coals ($R^2 = 0.81$, linear and $P < 0.05$). This indicates that the moisture plays a critical role affecting the methane sorption especially in low rank coals (Raniganj) than high rank coals (Jharia). Crosdale et al. (2008) studied the sorption behavior of sub-bituminous coals from Huntly Coalfield and found that sorption capacity increases non-linearly with the decrease in moisture content. However, as the moisture content varies within a narrow yet distinct range (Raniganj Coals: 2.6–4.6% and Barakar Coals: 0.5–1.7%), the sorption capacity (as received basis) shows a linear relation with moisture for respective set of coals, probably representing a portion of the non-linear curve as discussed by Crosdale et al. (2008). A negative linear relation is also found by Levy et al. (1997) for Bowen basin Permian coals of Australia having C ranging between 82 and 92% (daf). Negative relationship for sorption capacity of coals under varying moisture conditions has also been found by Moore and Crosdale (2006); Crosdale et al. (2008) etc. Micropores available for methane sorption are occupied by the water/moisture and reduce the methane adsorption capacity (Yee et al., 1993). Experimental observation of Mavor et al. (1990) found a decrease in gas sorption capacity by almost 25% for 1% increase in moisture content for low rank sub-bituminous C coals from Powder River Basin and effect of moisture decreases with increase in coal rank.

5.3. Effect of ash on methane adsorption capacity

Most of the researchers have reported the negative impact of the ash content on gas sorption capacity (Yee et al., 1993; Clarkson and Bustin, 2011; Laxminarayana and Crosdale, 1999, 2002; Shan et al., 2018). The ash acts as a simple inert diluent as it reduces the site available for adsorption by reducing the organic matter having microporosity (Gunther, 1965; Yao et al., 2008; Li et al., 2015). Further, Feng et al. (2014) stated that clay and carbonates are the dominant minerals in coal that block the pores and affect the storage of methane in coal. Methane is adsorbed onto the organic surface rather than inorganic mineral surface, owing to which adsorption capacity reduces with the increase in mineral/ash content. Clay is the dominant mineral with few carbonates and silicates found in both the Raniganj and Barakar coals. In the present study authors have found (Fig. 13b) a statistically significant negative linear trend for both the Raniganj ($R^2 = 0.51$, $P < 0.05$) and Jharia coals ($R^2 = 0.47$, $P < 0.05$). Olajossy (2014) has found similar type of discrete relationship for the Polish coals. To decouple the grade and rank effect to observe the variation in sorption with ash content, sorption capacity at 3Mpa was plotted against ash. A weak negative linear relation ($R^2 = 0.45$, and $P < 0.05$) is found for low rank Raniganj coals and strong negative linear relation ($R^2 = 0.94$, and $P < 0.05$) for Barakar coals, and both are statistically significant (Fig. 13c).

5.4. Effect of volatile matter and fixed carbon on methane adsorption capacity

The volatile matters are the small molecular functional groups occurring as side chains of macromolecular structure in coal. Though VM does not contribute to the adsorption capacity, as a measure of rank, the decrease in VM indicates higher level of maturity and hence, increases in aromaticity with a resultant increase in the sorption capacity. The adsorption of methane in coal is mainly contributed by micropores present in coals (Liu, 2010). The volatile matter and normalized methane adsorption capacity at 3 MPa instead of Langmuir volume are plotted for dry ash free basis for comparison on a basis independent of moisture and inorganic matter. Fig. 14a clearly depicts that results are very much distinguishable for Raniganj and Barakar coals. A strong decreasing trend is observed for both Raniganj ($R^2 = 0.76$, $P < 0.05$) and Barakar ($R^2 = 0.81$, $P < 0.05$) coals at 5% level of significance. This is similar to the earlier observation of Mohanty et al. (2018) for the Raniganj coals. Beamish et al. (1998) had made a comparison between volatile matter (daf) vs Langmuir volume (daf), and found very similar distinguishable data points for the New Zealand and Australian coals. However, a weak relationship has been established by Faiz et al. (1992) for a set of Australian Permian coals.

The relationship between Langmuir volume and fixed carbon is well explained (Gurdal and Yalcin, 2000). The normalized methane adsorption capacity at 3 MPa against fixed carbon is plotted in Fig. 14b shows a strong positive relationship for both the Raniganj and Barakar coals. Both the data has been calculated on dry ash free basis to eliminate the effect of moisture and ash. Levy et al. (1997) have established similar positive relationship for Permian Bowen basin coals of Australia and found an increase of adsorption capacity by 3 cc/g per 10% increase of fixed carbon content for the fixed carbon range of 60–90%.

5.5. Effect of maceral composition on methane adsorption capacity

Macerals occur in association with each other, generally known as microlithotypes (Stach et al., 1982). Different microlithotypes have

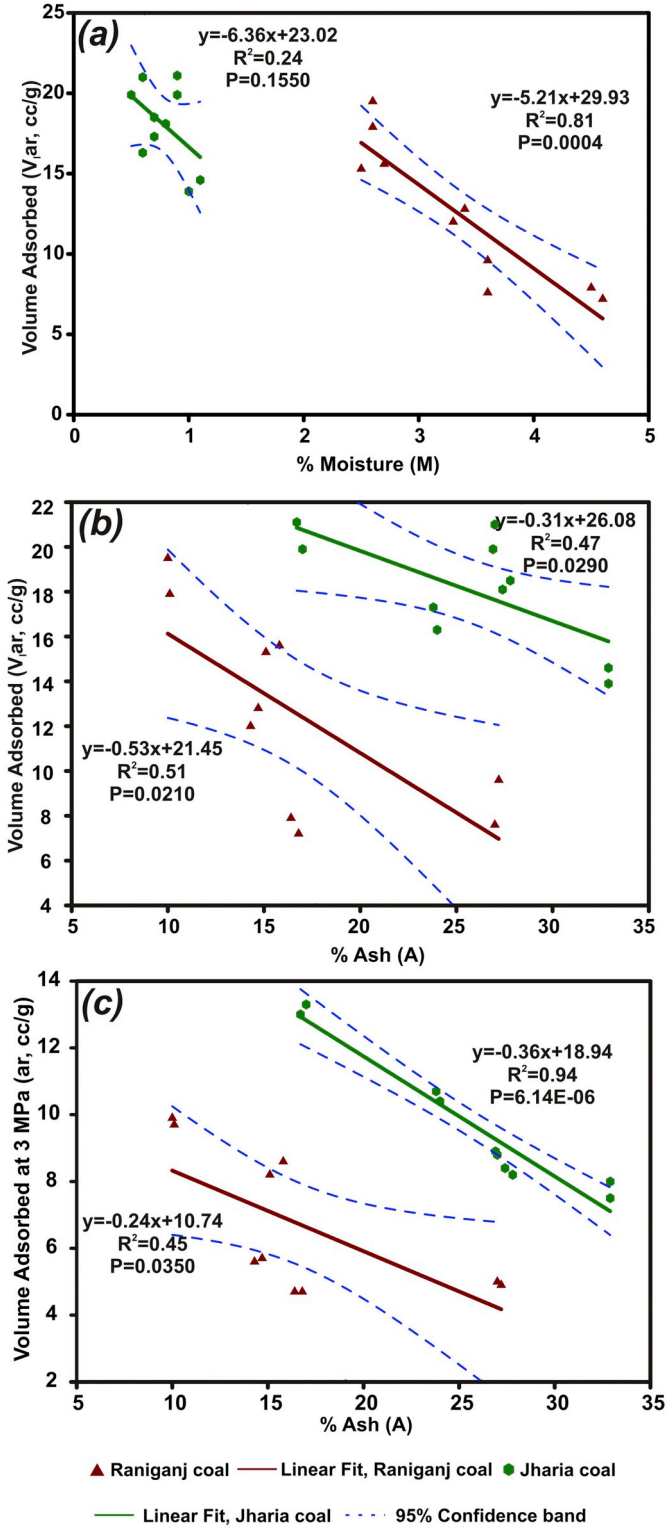

Fig. 13. Effect of *(a)* moisture content and *(b)* ash content on Langmuir Volume (V_L), and effect of (c) ash content on normalized methane adsorption capacity at 3 MPa for the coals of Raniganj Formation, Raniganj Sub-basin and Barakar Formation, Jharia Sub-basin.

different pore size and pore structure at the same rank and/or mineral content, which mainly control the methane storage capacity (Laxminarayana and Crosdale, 2002; Chattaraj et al., 2016). Maceral composition of the studied coals has been presented in section 4.2. The influence of macerals on CH_4 storage capacity is shown in Fig. 15 (a-c).

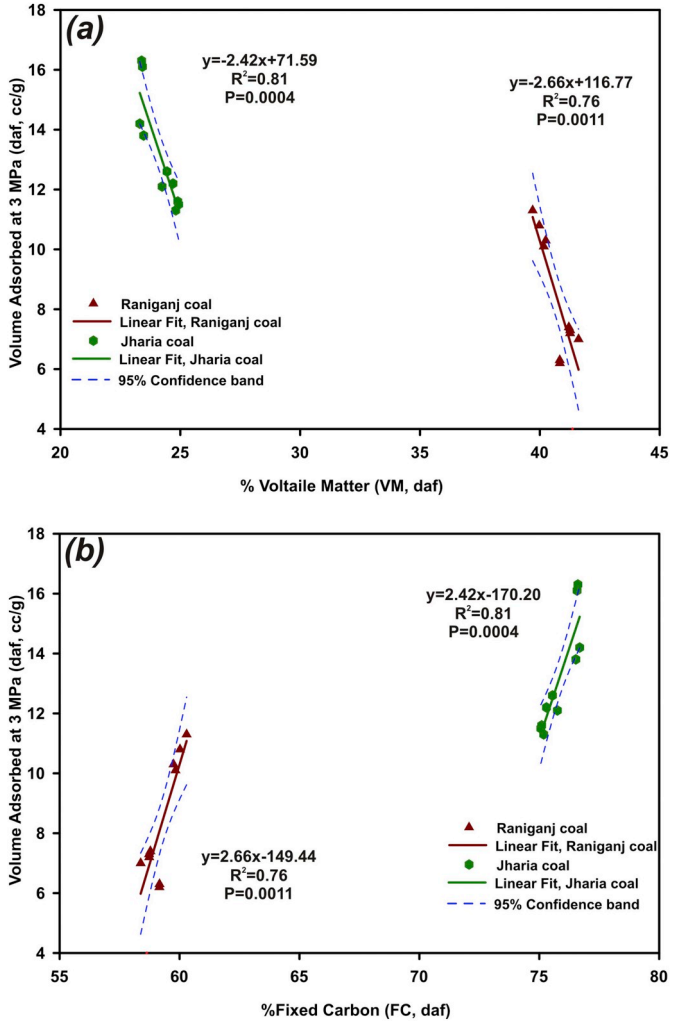

Fig. 14. Variation in normalized methane adsorption capacity at 3 MPa with (a) volatile matter (b) fixed carbon for the coals of Raniganj Formation, Raniganj Sub-basin and Barakar Formations, Jharia Sub-basin.

As the inorganic mineral matter of the coal has the negative effect on CH_4 storage capacity, for the better understanding of the effect of maceral composition Langmuir volume has been converted into the dry ash free (daf) basis whereas maceral percentage has been converted in to visible mineral matter free (mmf) basis. Many researchers have already discussed the control of maceral composition on adsorption capacity of coals from different basins (Ettinger et al., 1966; Faiz et al., 2007; Lamberson and Bustin, 1993; Bustin et al., 1995; Crosdale et al., 1998; Clarkson and Bustin, 1999; Shan et al., 2018). Most of the researchers have found a positive relationship with the vitrinite content (ref). Present study also shows a statistically significant increasing trend for Langmuir volume (V_L)with vitrinite content (Fig. 15a; Raniganj coals- $R^2 = 0.88$, $P < 0.05$; Barakar coals- $R^2 = 0.87$, $P < 0.05$), negative trend with inertinite (Fig. 15b; $R^2 = 0.62$, $P < 0.05$ and $R^2 = 0.45$, $P < 0.05$ for both Raniganj and Barakar coals respectively) and with liptinite (Fig. 15c; $R^2 = 0.37$, and $R^2 = 0.47$, $P < 0.05$ for both Raniganj and Barakar coals respectively). As vitrinite contain higher microsporosity compared to other maceral groups, the adsorption capacity increases with increase in vitrinite content (Laxminarayana and Crosdale, 1999). The difference in trend for coals from two sub-basins indicate that they have different types of precursor organic matter and have evolved through different degrees of thermal maturity. However, Carroll and Pashin (2003) and Mastalerz et al. (2004) did not find any trend between maceral composition and CH_4

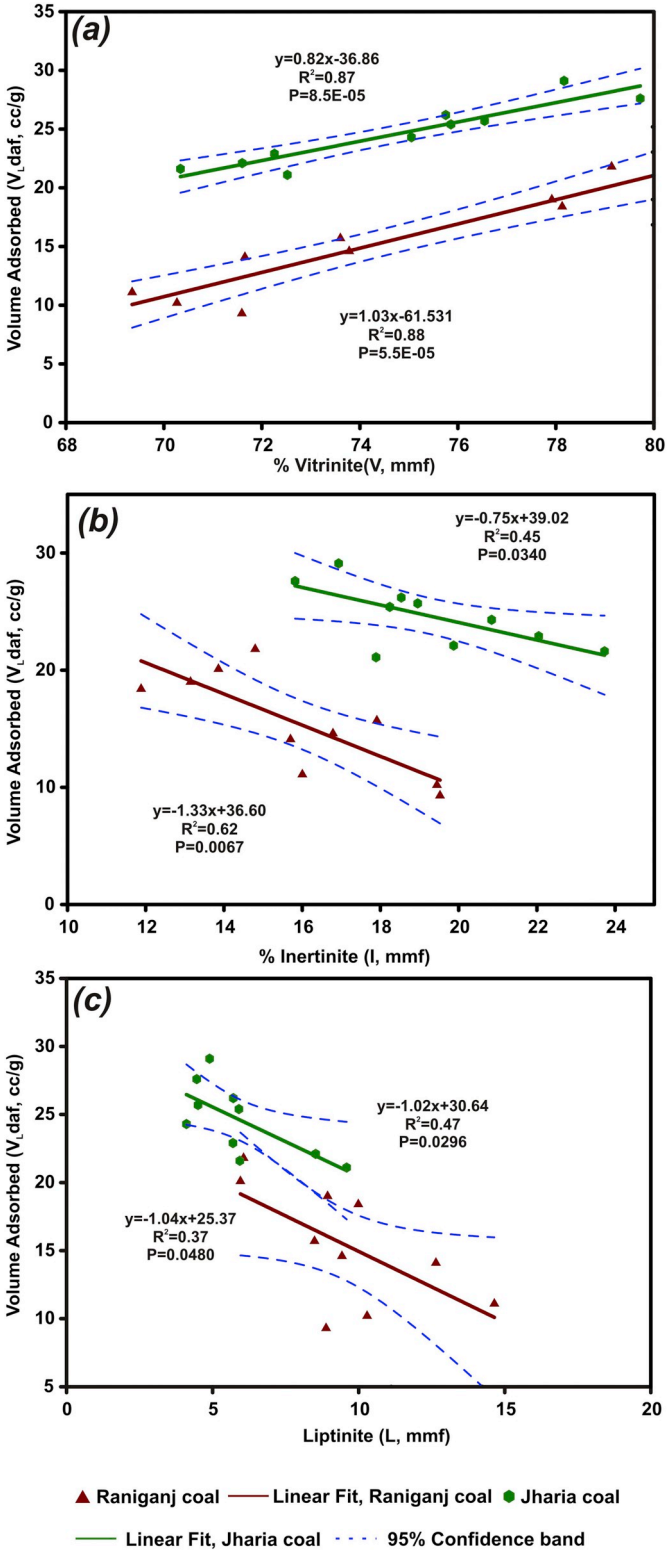

Fig. 15. Relationship between (a) vitrinite (V) content; (b) inertinite (I) content; (c) liptinite (L) content and Langmuir volume (V_L) for the coals of Raniganj Formation, Raniganj Sub-basin and Barakar Formations, Jharia Sub-basin.

adsorption capacity for USA coals. Kiani et al. (2017) have shown that both the number of pores and rates of gas sorption increase with inertinite content though the relationship with inertinite content differed for coals from different basins.

5.6. Effect of rank on on methane adsorption capacity

Carbon is the most dominant organic component present in the coal. Its content in coal is dependent on the coal type, coal composition and degree of coalification. Adsorption of methane in the coalbed is reliant on the coal rank (vitrinite reflectance) and organic carbon content. Previous study shows that adsorption capacity increases with rank from sub-bituminous to anthracite (Kim, 1977; Yee et al., 1993). The methane generation during coalification peaks around medium volatile bituminous stage (Fig. 10). Storage capacity of methane increases as the level of maturation of coal increases (Levy et al., 1997; Larsen, 2004). The presence of pore water reduces the adsorption capacity either by blocking the path to or by occupying the adsorption sites within the coal matrix (Seewald and Klein, 1986). In case of low to middle rank coals, adsorption capacity steadily decreases with moisture due to occupancy of the available adsorption sites by the moisture. In high rank coals, though there is roughly the same trend between Langmuir volume and moisture, the rate of variation is less owing to lesser moisture content. However, progressive aromatization results in increased microporosity and carbon content that primarily guides the sorption in high rank coals (Guo and Guo, 2018). Although the overall porosity declines, an increase in sorption is caused by the increase in microporosity along the coalification path as the small pores have higher surface area available for monolayer adsorption (Gan et al., 1972).

The rank, represented by vitrinite reflectance and organic carbon (C_{dmmf}), plays a dominant role in methane sorption of coal over the entire rank range (Mavor et al., 1990). Hence, all the datasets were plotted together to observe the overall variation in sorption capacity with rank change for the suites of coals. The 2nd order polynomial equation is fitted to the datasets which shows the regression coefficient of 0.70 and 0.60 for the curve of Langmuir volume (Fig. 16a) and methane adsorption capacity at 3 MPa (Fig. 16c) with carbon content. The P- values for both the model are found to be within required significance level. Laxminarayana and Crosdale (2002) found similar relationship between vitrinite reflectance and sorption capacity of Indian coals. For Australian Bowen basin coal Laxminarayana and Crosdale (1999) found discrete 2nd order polynomial relationship between vitrinite reflectance and sorption capacity. However, Bustin and Clarkson (1998) has stated that there are no significant linear or nonlinear relationship between adsorption capacity and coal rank. Most of the researchers have found a strong positive relationship between these parameters (Gurdal and Yalçin, 2000; Mastalerz et al., 2004; Fu et al., 2007; Wang et al., 2011; Guo and Guo, 2018). The relationships between Langmuir volume (V_L)/adsorption capacity at 3 MPa and vitrinite reflectance (R_r) for the set of Indian coals are shown in Fig. 16(b &d) which shows almost similar trend with the R^2 of 0.79 and 0.77.

The gas content and reflectance data (Table 5) of different coal seams of Raniganj Formation, Raniganj Sub-basin (Mohanty et al., 2018) and Barakar Formations, Jharia Sub-basin (Pal et al., 2015) indicates that the coal seams have significant potential for CBM resources.

5.7. Formation of predictive model using multiple regression analysis

In the next step, multiple regression analyses were carried out to observe the main and coupled effect of ash (%A), moisture (%M), carbon (%C), and reflectance (%R_r). Multiple regression analysis can be defined as the statistical procedure for analysis of data considering more than one type of measurement or observation (Schneider et al., 2010). This analysis is also significant in case when dependent variable (s) depend on a combination of independent variables (Mahmood and Elektorowicz, 2017). The regression model is mainly produced by parameter estimation, which represent regression coefficient for each independent variable (Permai and Tanty, 2018). Table 6 and Table 7 summarises the results of regression coefficient and corresponding P-values for the main effects and interaction effects of input variables towards output variable "Langmuir volume (V_L)", respectively. The

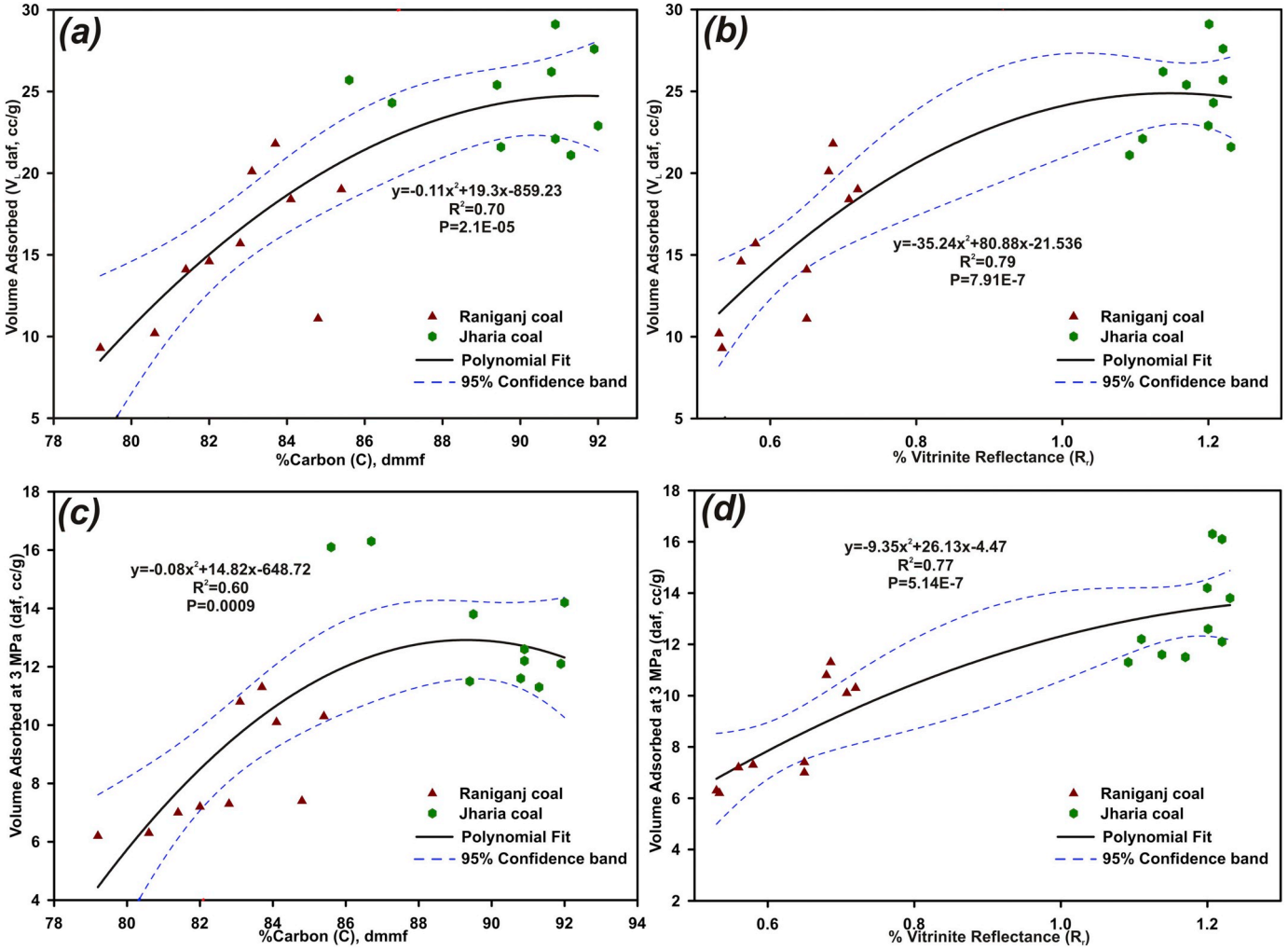

Fig. 16. Variation of *(a)* Carbon content (C) and *(b)* vitrinite reflectance (R_r) with Langmuir volume (V_L),and variation of *(c)* Carbon content (C) and *(d)* vitrinite reflectance (R_r) with normalized methane adsorption capacity at 3 MPa for the coals of Raniganj Formation, Raniganj Sub-basin and Barakar Formations, Jharia Sub-basin.

Table 5
Gas content data of different coal seams of Raniganj Formation, Raniganj Sub-basin and Barakar Formations, Jharia Sub-basin (Sources: Pal et al., 2015 and Mohanty et al., 2018).

Raniganj Coals, Raniganj Sub-Basin (Mohanty et al., 2018)				Barakar Coals, Jharia Sub-Basin (Pal et al., 2015)			
Seam	Depth (m)	% R_r	Gas Content (daf, cc/g)	Seam	Depth (m)	% R_r	Gas Content (daf, cc/g)
R-X (A)	267.25	0.61	3.24	B-XVIIIT (A)	214.58	1.27	11.27
R-VIII (A)	425.49	0.66	5.03	B-XVII	282.78	1.21	11.14
R-VI (A)	632.29	0.71	7.86	B-XVI	490.08	1.56	11.12
R-IV (A)	892.81	0.73	10.69	B-XV	526.05	1.46	11.12
R-III (A)	983.86	0.80	7.69	B-XIV	540.92	1.41	11.28
R-II (A)	1098.04	0.86	8.86	B-XIII	561.28	1.75	11.17
R-I (A)	1122.95	0.84	11.40	B-XII	631.48	1.40	11.21
				B-XI	639.88	1.48	11.23
				B-X	663.78	1.48	11.12
				B-IX	674.88	1.41	11.23
				B-VIII	720.58	1.51	11.23
				B-VII/VI/V	762.08	–	11.11
				B-IV	802.28	–	11.21
				B-III	831.18	1.67	11.12
				B-II	842.28	1.71	11.20
				B-I	1214.52	–	–

results show that all the input variables have negative influence on the V_L. The variable "moisture" has a highest negative influence on the V_L (ar) and V_L (daf) for the 1st type of coal with the coefficient value of −109.3, and − 132.7, respectively. Similarly, for the second case, the parameters were obtained as −19.53 and − 21.95. The coefficient values for the moisture are statistically significant at 5% level of significance, which reveals that the moisture is the significant predictor of the V_L. The ash, carbon, and reflectance also tend to decrease the value

Table 6
Results of main effect of input variables on the V_L.

Main effect	V_L, ar		V_L, daf	
	Coefficient	P-value	Coefficient	P-value
Ash (% A)	-10.510	0.078	-10.940	0.160
Moisture (%M)	-109.300	0.013*	-132.700	0.022*
Carbon (%C)	-2.520	0.061	-2.770	0.114
Ash (%A)	-1.190	0.504	-0.450	0.852
Moisture (%M)	-19.530	0.016*	-21.950	0.040*
Reflectance (%R_r)	-24.900	0.271	-22.500	0.460

Ash = %A, Moisture = %M, Carbon = %C, Reflectance = R_r

Table 7
Results of second and third order interaction effect of input variables on the V_L.

Interaction Parameters		Coefficient		P-Value	
		V_L ar	V_L daf	V_L ar	V_L daf
% A* %M	For Carbon	5.370	6.550	0.020*	0.031*
	For Reflectance	0.769	0.855	0.068	0.129
%A* %R_r		1.370	1.180	0.338	0.544
%M* % R_r		29.200	35.900	0.052	0.076
%A* %C		0.118	0.127	0.077	0.144
% M* %C		1.249	1.537	0.016*	0.024*
% A* %M* %C		−0.063	−0.078	0.019*	0.027*
%A* %M* %R_r		−1.250	−1.606	0.055	0.069

Where, * o n *P*-values indicates 5% significance level.

of V_L, but these are not significant at 5% significance level. The coefficients of reflectance were obtained as −24.9, and − 22.5 for V_L (ar) and V_L (daf), but it is associated with the errors of 27.1% and 46.0% respectively. Therefore, the negative effect of reflectance may not be true for all of the cases and it may exhibit different trend for different datasets.

Table 7 reveals the results of second and third order interaction effects of ash, moisture, carbon, and reflectance on the V_L. It can be seen that all the second order interactions have a positive influence on the V_L. The interaction of %A* %M, and %M* %C shows statistical significance, whereas rest of the second order interactions are statistically insignificant. The coefficient values for the third order interaction of %A* %M* %C and %A* %M* %R_r are obtained as −0.063 and − 1.25 for V_L(ar), and − 0.078 and − 1.606 for V_L (daf), respectively. It shows that the interaction of moisture with the ash and carbon tends to decrease the output variable significantly. The interaction of %A* %M* %R_r also diminishes the V_L, but this interaction is statistically insignificant.

From Table 6 and Table 7, it can be concluded that the variable 'moisture' is the most influencing parameter of V_L and, the interaction of moisture with ash and carbon can effectively control the variation in the V_L. Consequently, the predictive equations for V_L(ar) and V_L(daf) are given below:

$$V_{L\,(ar)} = 246 - 10.5A - 109.3M - 2.5C + 5.37A * M + 0.12A * C + 1.25M * C - 0.06A * M * C$$

And

$$V_{L\,(daf)} = 266 - 10.94A - 132.7M - 2.77C + 6.55A * M + 0.13A * C + 1.54M * C - 0.09A * M * C$$

6. Conclusions

Sorption characteristics of world coals are extensively studied by various researchers. The phenomenon is primarily guided by pore size and structure and distribution that varies with rank, and also affected by grade and coal type. For the present investigation, coals of younger Raniganj Formation, Raniganj Sub-basin and older Barakar Formation, Jharia Sub-basin of Damodar Valley Basin of India have been investigated under same experimental conditions to understand the influence of grade, coal type and thermal maturity on methane sorption capacity of the suite of coals. Following conclusions were drawn from the study:

- The Raniganj Coals of Raniganj Sub-basin are sub-bituminous to high volatile bituminous type whereas the Barakar coals of Jharia Sub-basin are high volatile bituminous to medium volatile bituminous type.
- van Krevelen diagram reveals that both the Raniganj and Barakar coals fall mostly within kerogen Type-III with few Barakar coals tending towards kerogen Type-IV.
- The Raniganj coals falls in wet gas maturity stage approaching early-thermogenic methane generation whereas Barakar coals falls in condensate gas stage approaching peak-thermogenic methane generation.
- The effect of moisture is prominent in low rank Raniganj coals than high rank Barakar coals and shows decrease in sorption capacity with increase in moisture content.
- Low volatile matter content of Barakar coals of Jharia compared to Raniganj coals of Raniganj may be attributed to the maturity of Barakar coals that approaches towards second stage of coalification jump. This indicates higher degree of aromatization of Barakar coals thereby increasing the microporosity. This provides more sites for sorption and is evident from the higher methane sorption capacity for these suites of coals.
- The methane sorption capacity shows a strong positive relationship with vitrinite content and, negative relation with inertinite content and liptinite content. This corroborates the earlier studies that showed the increase in microporosity with vitrinite content thereby providing more sites for methane sorption.
- The methane sorption shows a strong rank dependence as evident from a strong positive relationship between carbon content/vitrinite reflectance and Langmuir volume for the studied coals. The sorption capacity of Barakar coals is relatively higher than the Raniganj coals because of the differential rank enhancement due to different burial and thermal history. Predictive model equations based on multiple regression analyses are developed for Damodar basin coals for determination of sorption from carbon, ash and moisture data.

Acknowledgements

DM is thankful to SERB and CSIR for financially supported through Grant No. SR/S4/ES- 591/2011 and Grant No. ESC – 0302, respectively. SC acknowledges Secondary Funding Source: Council of Scientific & Industrial Research (CSIR) for funding fellowship through File No. 31/22 (0028)/2017-EMR-I and ESC – 0302. Thanks are due to the Director, CSIR-Central Institute of Mining and Fuel Research, India for his kind permission to publish the paper. Authors express their indebt gratitude to Dr. C. Özgen Karacan, Editor-in-Chief, Dr. Sedat Inan and one anonymous reviewer for their critical reviewing and constructive suggestions on the previous version of the manuscript, which has helped improving the paper. Special thanks to Dr. Subhabrata Paul of IIT Kharagpur for his suggestions for statistical analysis of the experimental data.

References

Arri, L., Yee, D., Morgan, W., Jeansonne, M., 1992. Modeling Coalbed methane production with Binary Gas Sorption. In: SPE Rocky Mountain Regional Meeting, Casper, WY, USA, 18–21 May 1992, 18–21, SPE-24363-MS.

ASTM D1412/D1412M, 2015. Standard Test Method for Equilibrium Moisture of Coal at 96 to 97 Percent Relative Humidity and 30°C. ASTM International, West Conshohocken, PA, pp. 5. https://doi.org/10.1520/D1412_D1412M-15.

ASTM D2013/D2013M, 2018. Standard Practice for Preparing Coal Samples for Analysis.

19428-2959. ASTM International, West Conshohocken, PA, pp. 12. https://doi.org/10.1520/D2013_D2013M-18. United States.
ASTM D3172, 2013. Standard Practice for Proximate Analysis of Coal and Coke. ASTM International, West Conshohocken, PA, pp. 2. https://doi.org/10.1520/D3172.
ASTM D3176, 1979. Standard Method for Ultimate Analysis of Coal and Coke [C, H, S, N, O, Ash], 409–412. ASTM International, West Conshohocken, PA, pp. 4. https://doi.org/10.1520/D3176-15.
ASTM D388, 2018. Standard Classification of Coals by Rank. 5 ASTM International, West Conshohocken, PA. https://doi.org/10.1520/D0388-18.
Bandopadhyay, A.K., Mohanty, D., 2014. Variation in hydrogen content of vitrinite concentrates with rank advance. Fuel 134, 220–225. https://doi.org/10.1016/j.fuel.2014.05.057.
Beamish, B., Laxminarayana, C., Crosdale, P.J., 1998. Contrasts in methane sorption properties between New Zealand and Australian coals. In: N. Aziz (Ed.), Coal 1998: Coal Operators' Conference. University of Wollongong & the Australasian Institute of Mining and Metallurgy, pp. 561–565.
Busch, A., Gensterblum, Y., 2011. CBM and CO_2-ECBM related sorption processes in coal: a review. Int. J. Coal Geol. 87, 49–71.
Bustin, R.M., Clarkson, C.R., 1998. Geological controls on coalbed methane reservoir capacity and gas content. Int. J. Coal Geol. 38, 3–26.
Bustin, R.M., Clarkson, C.R., Levy, J., 1995. Coalbed methane adsorption of coals of the Bulli and Wongawill seams, southern Sydney Basin: Effects of maceral composition. In: 29th Newcastle Symposium on Advances in the Study of the Sydney Basin, Newcastle NSW, Australia, Department of Geology. The University of Newcastle, NSW, pp. 22–28.
Carroll, R.E., Pashin, J.C., 2003. Relationship of sorption capacity to coal quality: CO2 sequestration potential of coalbed methane reservoirs in the Black Warrior Basin. In: Proceedings of the International Coal Bed Methane Symposium, pp. 1–11.
Casshyap, S.M., Tewari, R.C., 1987. Depositional model and tectonic evolution of Gondwana Basins. Palaeobotanist 36, 59–66.
Chandra, D., 1962. Reflectance and microstructure of weathered coals. Fuel 41, 155–163.
Chandra, K., 1997. Alternative hydrocarbon resources in the next millennium, Geohorizons, v.2, no.2. Levine, J.R., 1993. In: Law, B.E., Rice, D.D. (Eds.), Coalification: The Evolution of Coal as Source Rock and Reservoir Rock for Oil and Gas. Studies in Geology Series, Tulsa, pp. 39–77.
Chandra, D., Chakrabarti, N.C., 1989. Coalification trends in Indian coals. In: Coal: Classification, Coalification, Mineralogy, Trace-element Chemistry, and Oil and Gas Potential. Int. J. Coal Geol. 13. pp. 413–435.
Chattaraj, S., Mohanty, D., Kumar, T., Halder, G., 2016. Thermodynamics, kinetics and modeling of sorption behavior of coalbed methane – a review. J. Unconv. Oil Gas Resour. 16, 14–33. https://doi.org/10.1016/j.juogr.2016.09.001.
Choudhury, N., Mohanty, D., Boral, P., Kumar, S., Hazra, S.K., 2008. Microscopic evaluation of coal and coke for metallurgical usage: a case study. Curr. Sci. 94-1, 74–81.
Clarkson, C.R., Bustin, R.M., 1999. The effect of pore structure and gas pressure upon the transport properties of coal: a laboratory and modeling study. 2. Adsorption rate modeling. Fuel 78, 1345–1362.
Clarkson, C.R., Bustin, R.M., 2011. Coalbed methane: current field-based evaluation methods. SPE Reserv. Eval. Eng. 14, 60–75.
Cornford, C., 1998. Source rocks and hydrocarbons of the North Sea. In: Glennie, K.W. (Ed.), Petroleum Geology of the North Sea: Basic Concepts and Recent Advances, 4th ed. Oxford, Blackwell, pp. 376–462.
Crosdale, P.J., Beamish, B.B., Valix, M., 1998. Coalbed methane sorption related to coal composition. Int. J. Coal Geol. 35 (1–4), 147–158.
Crosdale, P.J., Moore, T.A., Mares, T.E., 2008. Influence of moisture content and temperature on methane adsorption isotherm analysis for coals from a low-rank, biogenically-sourced gas reservoir. Int. J. Coal Geol. 76, 166–174. https://doi.org/10.1016/j.coal.2008.04.004.
DGH, 2019. Directorate General of Hydrocarbons. website. www.dghindia.org/index.php/story_details?story=4&heading=Award%20of%20Blocks%20Under%20CBM%20-%20IV%20Bidding%20Round.
Dutta, P., 2002. Gondwana Lithostratigraphy of Peninsular India. Gondwana Res. 5, 540–553.
Ettinger, I., Eremin, I., Zimakov, B., Yanovskaya, M., 1966. Natural factors influencing coal sorption properties. I. Petrography and sorption properties of coals. Fuel 45, 267–275.
Faiz, M., Aziz, N.I., Hutton, A.C., Jones, B.G., 1992. Porosity and Gas sorption capacity of some eastern Australian coals in relation to coal rank and composition. In: Coalbed Methane Symposium, Townsville, Australia. Vol. 11 19–21 November.
Faiz, M., Saghafi, A., Sherwood, N., Wang, I., 2007. The influence of petrological properties and burial history on coal seam methane reservoir characterization, Sydney Basin, Australia. Int. J. Coal Geol. 70 (1–3), 193–208.
Feng, Y., Yang, W., Chu, W., 2014. Contribution of ash content related to methane adsorption behaviors of bituminous coals. Int. J. Chem. Eng. 2014 (11), 956543. https://doi.org/10.1155/2014/956543.
Fox, C.S., 1930. The Jharia coalfield. In: Memoir Geological Survey of India. vol. 56. GSI, Kolkata, India, pp. 255.
Fu, X.H., Qin, Y., Wei, C.T., 2007. Coalbed Methane Geology. China University of Mining and Technology Press, Xuzhou, pp. 1–273 (in Chinese).
Gan, H., Nandi, S.P., Walker Jr., P.L., 1972. Nature of the porosity in American coals. Fuel, 51, 272-277. 2002 In: Gluskoter, H., Mastalerz, M., Stanton, R. (Eds.), The Potential for Carbon Dioxide Sequestration in Coal Beds: New Evidence from Methane and Carbon Dioxide Adsorption Analyses of Coals from Lignite to Anthracite. North-Central Section (36th) and Southeastern Section (51st), GSA Joint Annual Meeting Lexington, Kentucky, April 3–5.
Gunther, J., 1965. Etude de la Liaison Gaz-Charbon (Investigation of the Gas-Coal Bond). vol. 47. Revue del'Industric Mineralc, pp. 693–708.
Guo, D., Guo, X., 2018. The influence factors for gas adsorption with different ranks of coals. Adsorpt. Sci. Technol. 36 (3–4), 904–918.
Gurdal, G., Yalcin, M.N., 2000. Gas adsorption capacity of carboniferous coals in the Zonguldak Basin (NW Turkey) and its controlling factors. Fuel 79, 1913–1924.
Hall, F.E., Chunhe, Z., Gasem, K.A.M., Robinson, R.L., Yee, D., 1994. Adsorption of pure CH_4, N_2, and CO_2 and their binary mixtures on wet Fruitland coal. In: SPE-29194, Eastern Regional Conference and Exhibition, Charleston, WV, USA. 8–10 November, pp. 329–344.
Hogg, R.V., McKean, J.W., Craig, A.T., 2005. Introduction to Mathematical Statistics. Pearson, Boston, pp. 762.
Hunt, J.M., 1996. In: Freeman, W.H. (Ed.), Petroleum Geochemistry and Geology, 2nd ed. .
ISO 7404-2, 1985. Methods of Petrographic Analysis of Coal. Part 2: Methods for Preparing Coal Samples. vol. 12https://doi.org/10.3403/30145807.
ISO 7404-3, ISO, 1994. Methods for the petrographic analysis of bituminous coal and anthracite. In: Part 3: Method of Determining Maceral Group Composition, pp. 18. https://doi.org/10.3403/30145810.
ISO 7404-5, 1994. Methods for the Petrographic Analysis of Bituminous Coal and Anthracite, Part 5: Method of Determining Microscopically the Reflectance of Vitrinite. pp. 14.
Jiménez, A., Iglesias, M.J., Laggoun-Defarge, F., Sua'rez-Ruiz, I., 1999. Effect of the increase in temperature on the evolution of the physical and chemical structure of vitrinite. J. Anal. Appl. Pyrolysis 50, 117–148.
Joubert, J.I., Grein, C.T., Bienstock, D., 1974. Effect of moisture on the methane capacity of American coals. Fuel 53, 186–191.
Juntgen, H., Karweil, J., 1966. Formation and Storage of Gas in Bituminous Coals: Part I & II: Erdol Und Kohle, Erdgas, Petrochemie. (v. 19, I/p. 251–258 & II/ p. 339–344).
Kiani, A., Sakurovs, R., Grigore, M., Sokolova, A., 2017. Gas sorption capacity, gas sorption rates and nanoporosity in coals. Int. J. Coal Geol. 200 (1), 77–86 December 2018.
Kim, A.G., 1977. Estimating the Methane Content of Bituminous Coalbeds from Adsorption Data. 8245. USBM Reports of Investigation, RI, pp. 22.
Kraiser, K.M., Sinha, D.K., Bagchi, S., 1964. Thermal gradients in Indian coalfields. Cent. Min. Res. Stn. Dhanbad Res. Ap. 15.
Lamberson, M.N., Bustin, R.M., 1993. Coalbed methane characteristics of Gates Formation coals, northeastern British Columbia: effect of maceral composition. AAPG Bull. 77, 2062–2076.
Larsen, J.W., 2004. The effects of dissolved CO2 on coal structure and properties. Int. J. Coal Geol. 57, 63–70.
Larsen, J.W., Lee, D., Shawver, S.E., 1986. Coal macromolecular structure and reactivity. Fuel Process. Technol. 12, 51–62.
Laxminarayana, C., Crosdale, P.J., 1999. Role of coal type and rank on methane sorption characteristics of Bowen Basin, Australia coals. Int. J. Coal Geol. 40, 309–325.
Laxminarayana, C., Crosdale, P.J., 2002. Controls on methane sorption capacity of Indian coals. AAPG Bull. 86, 201–212.
Levine, J.R., 1993. Coalification: The evolution of coal as source rock and reservoir. In: Law, B.E., Rice, D.D. (Eds.), Hydrocarbons from Coal. 38. American Association of Petroleum Geologists, AAPG Studies in Geology, pp. 39–77.
Levy, J., Day, H., Killingley, J.S., 1997. Methane capacities of Bowen basin coals related to coal properties. Fuel 76 (9), 813–819.
Li, Q.Z., Lin, B.Q., Wang, K., Zhao, M.Z., Ruan, M.L., 2015. Surface properties of pulverized coal and its effects on coalmine methane adsorption behaviors under ambient conditions. Powder Technol. 270, 278–286.
Liu, P., 2010. A Research on the Methane Adsorption/Desorption in the Mid and High Rank Bituminous. The master degree thesis of Xi' An university of science and technology, China (in Chinese with English abstract).
Mahmood, Ali A., Elektorowicz, M., 2017. Multiple Regression Analysis of Unconfined Compression Strength of Mine Tailings Matrices. In: MATEC Web of Conferences. 103, 07010 (2017). https://doi.org/10.1051/matecconf/201710307010.
Mastalerz, M., Gluskoter, H., Rupp, J., 2004. Carbon dioxide and methane sorption in high volatile bituminous coals from Indiana, USA. Int. J. Coal Geol. 40, 309–325.
Mavor, M.J., Owen, L.B., Pratt, T.J., 1990. Measurement and evaluation of coal sorption isotherm data. In: SPE 20728, SPE 65th Annual Technical Conference and Exhibition, New Orleans, Louisiana, September 23–26.
Michalski, S.R., Custer Jr., E.S., Munshi, P.L., 1997. Investigation of the Jharia coalfield mine fires - India. Proc. Am. Soc. Min. Reclam. 211–223. https://doi.org/10.21000/JASMR98010211.
Mohanty, D., 2019. Coal Seam Gas - Evaluation, Extraction and Environmental Issues (chapter 7). In: Kundu, S.N., Nawaz, M. (Eds.), Earth, Energy, and Environment. Apple Academic Press (in press, ISBN: 9781771887632).
Mohanty, D., Chattaraj, S., Singh, A.K., 2018. Influence of coal composition and maturity on methane storage capacity of coals of Raniganj coalfield, India. Int. J. Coal Geol. 196, 1–18.
Moore, T., Crosdale, P., 2006. The effect of moisture and temperature on adsorption isotherms of a low-rank coal: Implications for reservoir modeling. In: 2006 International Coalbed Methane Symposium, Tuscaloosa, Alabama.
Mu, F., Zhong, W., Zhao, X., Che, C., Chen, Y., Zhu, J., Wang, B., 2015. Strategies for the development of CBM gas industry in China. Natural Gas Ind. B 2 (4), 383–389. https://doi.org/10.1016/j.ngib.2015.09.013.
Murray, D.K., 1991. Coal bed methane; natural gas resources from coal seams. In: Peters, C. (Ed.), Geology in Coal Resource Utilization, Tech Books, United States, pp. 97–103.
Olajossy, A., 2014. The influences of the rank of coal on methane sorption capacity in coals. Arch. Min. Sci. 59 (2), 509–516.
Pal, P.K., Paul, S., Chatterjee, R., 2015. Estimation of In-situ stress and coal bed methane potential of coal seams from analysis of well logs, ground mapping and laboratory data in central part of Jharia Coalfield—An overview. In: Mukherjee, S. (Ed.),

Petroleum Geosciences: Indian Contexts. Springer Geology, pp. 143–173. https://doi.org/10.1007/978-3-319-03119-4_6.
Patel, R.C., Sinha, H.N., Kumar, B.A., 2014. Basin provenance and post-depositional thermal history along the continental P/T boundary of the Raniganj basin, eastern India: Constraints from apatite fission track dating. J. Geol. Soc. India 83 (4), 403–413.
Permai, S.D., Tanty, H., 2018. Linear regression modeling using Bayesian approach for energy performance of residential building. Proc. Comp. Sci. 135, 671–677. https://doi.org/10.1016/j.procs.2018.08.219.
Peters, K.E., Cassa, M.R., 1994. Applied Source-Rock Geochemistry. In: Magoon, L.B., Dow, W.G. (Eds.), The Petroleum System. From Source to Trap. American Association of Petroleum Geologists, Tulsa, pp. 93–120.
Raja Rao, C.S., 1983. Coalfields of India Vol. III Coal Resources of Madhya Pradesh and Jammu and Kashmir. In: Bulletin of Geological Survey of India Series A. 45.
Rice, D.D., 1993. Composition and origins of coalbed gas. In: Law, B.E., Rice, D.D. (Eds.), Hydrocarbons from Coal.: AAPG Studies in Geology. 38. American Association of Petroleum Geologists, Tulsa, Oklahoma, pp. 159–184.
Schneider, A., Hommel, G., Blettner, M., 2010. Linear Regression Analysis Part 14 of a Series on Evaluation of Scientific Publications. Dtsch. Arztebl. Int. 107 (44), 776–782. https://doi.org/10.3238/arztebl.2010.0776.
Seewald, H., Klein, J., 1986. Methansorption an steinkohle und kennzeichnung der porenstruktur. Glückauf-Forschungshefte 47 (3), 149–156.
Shan, C., Zhang, T., Liang, X., Zhang, Z., Zhu, H., Yang, W., Zhang, K., 2018. Influence of chemical properties on CH4 adsorption capacity of anthracite derived from southern Sichuan Basin, China. Mar. Pet. Geol. 89 (Part – 2), 387–401. https://doi.org/10.1016/j.marpetgeo.2017.10.008.
Srivastava, R.K., Rao, N.V.C., Sinha, A.K., 2009. Cretaceous potassic intrusives with affinities to aillikites from Jharia area: Magmatic expression of metasomatically veined and thinned lithospheric mantle beneath Singhbhum Craton, Eastern India. Lithos 112, 407–418.
Stach, E., Mackowsky, M.T., Teichmuller, M., Taylor, G., Chandra, D., Teichmuller, R., 1982. Stach's Textbook of Coal Petrology. GebruderBorntraeger, Berlin, pp. 565.
Tissot, B.P., Welte, D.H., 1984. Petroleum Formation and Occurrence, 2nd ed. Springer-Verlag, Berlin, pp. 699.
Tissot, B., Durand, B., Espitalie, J., Combaz, A., 1974. Influence of the nature and diagenesis of organic matter in the formation of petroleum. Am. Assoc. Pet. Geol. Bull. 58, 499–506.
Togunwa, O.S., Abdullah, W.H., Hakimi, M.H., Barbeito, P.J., 2015. Organic geochemical and petrographic characteristics of Neogene organic-rich sediments from the onshore West Baram Delta Province, Sarawak Basin: Implications for source rocks and hydrocarbon generation potential. Mar. Pet. Geol. 63, 115–126.
Towler, B., Firouzi, M., Underschultz, J., Rifkin, W., Garnett, A., Schultz, H., Esterle, J., Tyson, S., Witt, K., 2016. An overview of the coal seam gas developments in Queensland. J. Natural Gas Sci. Eng. 31, 249–271. https://doi.org/10.1016/j.jngse.2016.02.040.
Van Krevelen, D.W., 1993. Coal; Typology-Chemistry-Physics-Constitution, 3rd ed. Elsevier, Amsterdam, pp. 979 Coal.
Veevers, J.J., Tiwari, R.C., 1995. Gondwana master basin of Peninsular India between Tethys and interior of the Gondwanaland province of Pangea. Mem. Geol. Soc. Am. Bull. 187, 1–72.
Walters, C.C., 2006. Chapter-2: The Origin of Petroleum. In: Hsu, C.S., Robinson, P.R. (Eds.), Practical Advances in Petroleum Processing. Springer, New York, NY, pp. 79–101. https://doi.org/10.1007/978-0-387-25789-1_2.
Wang, K.X., Fu, X.H., Qin, Y., Santigie, K.S., 2011. Adsorption characteristics of Lignite in China. J. Earth Sci. 22 (3), 371–376.
Yalçin, E., Durucan, S., 1991. Methane capacities of Zonguldak coals and the factors affecting methane adsorption. Min. Sci. Technol. 13, 215–222.
Yao, Y.B., Liu, D.M., Tang, D.Z., Tang, S.H., Huang, W.H., 2008. Fractal characterization of adsorption-pores of coals from North China: an investigation on CH_4 adsorption capacity of coals. Int. J. Coal Geol. 73, 27–42.
Yee, D., Seidle, J.P., Hanson, W.B., 1993. Gas sorption on coal and measurement of gas content. In: Law, B.E., Rice, D.D. (Eds.), Hydrocarbons from Coal. AAPG Studies in Geology, pp. 38.